Isolated Small Rat Hepatocytes Express both Annexin III and Terminal Differentiated Hepatocyte Markers, Tyrosine Aminotransferase and Tryptophan Oxygenase, at the mRNA Level

Shingo NIIMI,*[a] Masashi HYUGA,[a] Mizuho HARASHIMA,[b] Taiichiro SEKI,[b] Toyohiko ARIGA,[b] Toru KAWANISHI,[b] and Takao HAYAKAWA[c]

[a] *Division of Biological Chemistry and Biologicals, National Institute of Health Sciences; 1–18–1 Kamiyoga, Setagaya-ku, Tokyo 158–8501, Japan:* [b] *Department of Nutrition and Physiology, Nihon University College of Bioresource Sciences; Kameino Fujisawa 252–8510, Japan: and* [c] *Deputy Director, National Institute of Health Sciences; 1–18–1 Kamiyoga, Setagaya-ku, Tokyo 158–8501, Japan.*

Received August 4, 2004; accepted August 28, 2004; published online August 31, 2004

We recently showed that annexin III is expressed in isolated small rat hepatocytes but, not in parenchymal hepatocytes. In the present study, we used reverse transcription polymerase chain analysis to examine the annexin III mRNA level in isolated small rat hepatocytes and parenchymal hepatocytes. Annexin III mRNA was detected in isolated small hepatocytes, but not in isolated parenchymal hepatocytes, confirming the presence of annexin III expression in isolated small rat hepatocytes at the mRNA level and indicating that the absence of annexin III expression in isolated parenchymal hepatocytes is due to the absence of annexin III mRNA. Furthermore, we examined the mRNA level of tyrosine aminotransferase and tryptophan oxygenase, two terminally differentiated hepatocyte markers. mRNA for these markers was detected in both parenchymal hepatocytes and small hepatocytes.

Key words small rat hepatocyte; annexin III; differentiated hepatocyte phenotype

Small hepatocytes represent a minor population of cells that have been identified among cultured rat hepatocytes.[1—3] These cells have a high replication potential in some defined media[1—3] and differentiate into cells expressing either α1-antitrypsin, a differentiated hepatocyte marker protein, or biliary cell markers, such as BD1 and cytokeratins 7 and 19.[4] Small hepatocytes have also been found in normal and diseased human liver tissue,[5—7] can be cultured for more than 2 months, exhibit a high growth potential, and express differentiated hepatocyte phenotypes.[7] Therefore, human small hepatocytes are expected to be useful for cell therapy and as carrier cells for gene therapy in diseased liver.

Recently, we attempted to identify the proteins that are specifically expressed in small hepatocytes, but not in parenchymal hepatocytes. We discovered that annexin III is expressed in isolated small rat hepatocytes, but not in parenchymal hepatocytes.[8]

In the present study, we used reverse transcription polymerase chain reaction (RT-PCR) analysis to examine whether the difference in annexin III expression in these cells was due to a difference in mRNA levels. We also measured the mRNA levels of tyrosine aminotransferase (TAT) and tryptophan oxygenase (TO), two terminally differentiated hepatocyte markers, in isolated small rat hepatocytes to examine the hepatic differentiation state of the cells.

MATERIALS AND METHODS

Isolation of Small and Parenchymal Rat Hepatocytes Fractions of small hepatocytes and parenchymal hepatocytes were prepared from adult male Wistar strain rats (Japan SLC Co. ltd., Shizuoka, Japan) weighing 180—200 g by *in situ* perfusion of the liver with collagenase, followed by differential centrifugation[9] and Percoll gradient centrifugation using a method reported by Tateno *et al.*[10] All animal care and procedure protocols were approved by the institutional animal care committee.

RT-PCR Analysis Total RNA was extracted from cells washed with phosphate-buffered saline using a QuickPrep Total RNA Extraction kit (Amersham Biosciences, U.S.A) according to the manufacturer's protocol. Approximately 3 μg of RNA per sample was reverse-transcribed using a THERMOSCRIPT™ RT-PCR System (Invitrogen Life technologies, U.S.A.) and oligo(dT)$_{20}$ in a final volume of 40 μl, according to the manufacturer's protocol. Subsequently, 1 μl of cDNA corresponding to 12.5, 25 and 50 ng of template RNA was amplified using the THERMOSCRIPT™ RT-PCR System in a final volume of 20 μl per reaction, according to the manufacturer's protocol, for 20 cycles of denaturation for 30 s at 94 °C, annealing for 30 s at 60 °C, and polymerization for 1 min at 72 °C using each set of 5′ and 3′ primers (Table 1). The PCR products were separated on a 2% agarose gel, stained with SYBR Green 1, and visualized with a Fluoroimager 595 (Amersham Biosciences). The annexin III, TAT, and TO PCR product specificities were confirmed by DNA sequencing using an ABI Prism 377 Sequencer (Applied Biosystems, Foster City, CA, U.S.A.).

RESULTS AND DISCUSSION

Figure 1 shows the PCR products prepared from RNA derived from isolated small and parenchymal rat hepatocytes. The bands of the PCR products corresponded to those predicted by use of the respective primers. The PCR product of annexin III was detected in small hepatocytes, but not in parenchymal hepatocytes and its intensity increased depending on the amount of cDNA used. On the other hand, almost the same quantity of PCR products for albumin, a universal marker of hepatocytes, and glyceraldehyde 3-phosphate dehydrogenase (GAPDH), a housekeeping gene, were detected depending on the amount of cDNA used in both small hepatocytes and parenchymal hepatocytes.

* To whom correspondence should be addressed. e-mail: niimi@nihs.go.jp

Table 1. Sequence for PCR Primers in the 5′ to 3′ Orientation

Primer name	Accession No.	Nucleotide No.	Sequences	Predicted product size (bp)
Annexin III #1	NM 012823	64—83 1082—1063	TTGAGAGCAAGGTGGACAGC GCAGCTGTTGGAAGCCATCT	1019
Annexin III #2	NM 012823	672—691 1143—1124	CAAATTCACCGAGATCCTGT TGCTGGAGTGCTGTACGAAA	472
TAT	NM 012668	549—568 1098—1079	GTCTAGCTGTGTTGGCCAAT GTTCGCTGAAGGATGCTCTT	550
TO	M 55167	471—490 1157—1138	AGAGTACCTGTCTCCAGCAT ACCAGGTACGATGAGAGGTT	687
Albumin[11]	NM 134326	1080—1099 1728—1709	AAGGCACCCCGATTACTCCG TGCGAAGTCACCCATCACCG	649
GAPDH[12]	BC 059110	596—615 1047—1028	ACCACAGTCCATGCCATCAC TCCACCACCCTGTTGCTGTA	452

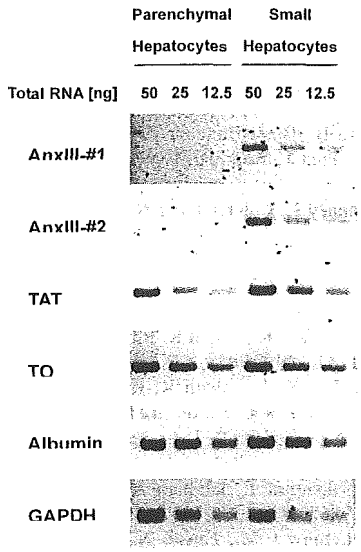

Fig. 1. RT-PCR Analysis of Annexin III, TAT and TO mRNA in Isolated Small Hepatocytes and Isolated Parenchymal Hepatocytes

Total RNA was extracted from isolated small rat hepatocytes and parenchymal hepatocytes and analyzed by RT-PCR, as described in the Materials and Methods section. The panel shows the RT-PCR results of a representative electrophoresis gel. The experiment was performed in triplicate.

These results indicate that annexin III mRNA is expressed in isolated small hepatocytes, but not in parenchymal hepatocytes. The absence of annexin III mRNA in the parenchymal hepatocytes was consistent with our previous findings[8] and the finding that annexin III mRNA was not detected in rat liver when examined using a Northern blot analysis.[13] The probable reason for the failure to detect annexin III mRNA in the latter study, in spite of the fact that small hepatocytes are a cell component of the liver, was the use of the whole liver in the analysis sample, reducing the detection sensitivity because the population of small hepatocytes in the liver is extremely small (less than 3% of the population of parenchymal hepatocytes in our preparation). On the other hand, a few reports have examined the expression patterns of other annexins in rat liver,[14,15] although no reports have examined the expression of any annexins in small hepatocytes, except for our previous findings.[8] The expression of annexin I and II was detected during the perinatal period, peaking at postnatal day 1 and gestational day 20, respectively, and reaching almost undetectable levels thereafter.[14,15] The expression of annexin V and VI was detectable at low levels during the fetal period and steadily detected at high levels thereafter.[15]

In contrast, the PCR products of TAT and TO were detected not only in the parenchymal hepatocytes, but also in the small hepatocytes. The intensity increased depending on the amount of cDNA used. As for the TAT and TO activities, it is uncertain whether the results of the present study reflect these activities in the small hepatocytes, since these enzyme activities in small hepatocytes have not been previously examined. In contrast, these activities have been detected in adult rat liver.[16—18] As the mRNA levels of TAT and TO in the parenchymal hepatocytes were almost the same as those in the small hepatocytes, it is likely that these activities are detectable in small hepatocytes at almost the same levels as those in parenchymal hepatocytes.

TAT expression is virtually absent in the fetus; the accumulation of mRNA is followed by an increase in enzyme activity after birth, when the transcription of the gene is activated.[16,19,20] TO expression is also virtually absent in the fetus; the accumulation of mRNA is followed by an increase in enzyme activity 14 d after birth, when the transcription of the gene is activated.[17,18,21,22] On the other hand, albumin mRNA expression has been detected in rat embryo on gestational day 9.5—10.5.[23] Based on their characteristic expression patterns, TAT and TO are used as terminal differentiated hepatocyte markers from hepatic progenitor cells or bone marrow-derived stem cells to hepatic cells.[11,24] In this respect, the present results showing the expression of TO and TAT mRNA in small rat hepatocytes were unexpected, because small hepatocytes are generally believed to be hepatic progenitor cells, based on their differential capacity as described in the introduction. This discrepancy between the results of the present study and the previous findings[4] suggests that the above findings may have derived from the experimental designs that were used, since isolated small hepatocytes were used for the RT-PCR analysis, but the phenotypes were examined in cultured small hepatocytes.[4] In this respect, it is noteworthy that all the small hepatocytes expressed α1-antitrypsin for at least for 4 h after plating, did not express α1-antitrypsin for the next 7 d of culture, and then expressed α1-antitrypsin after the 10 d of culture.[4] Since α1-antitrypsin mRNA is detected as early as gestational day 13 in rat embryo,[25] this marker is classified as an early differentiated hepatocyte marker. Therefore, this finding indicates that isolated small hepatocytes express an early differentiated hepatocyte marker, consistent with the present results. On the other hand, retrorsine-exposed rats can re-

place their entire mass after undergoing a 2/3 surgical partial hepatectomy (PH) through the emergence and expansion of a population of small hepatocyte-like progenitor cells (SHPCs).[26] SHPCs do not express mRNA for α1-antitrypsin 7 d after PH and exhibit mRNA expression patterns that are indistinguishable from those of fully differentiated hepatocytes 14 d after PH.[11] Similarly, SHPCs do not express TAT mRNA 5 d after PH, begin to express TAT mRNA 7 d after PH, and express a level of TAT mRNA comparable to that of fully differentiated hepatocytes 14 d after PH.[11] Therefore, the present results suggest that small hepatocytes initially dedifferentiate from cells expressing highly differentiated hepatocyte phenotypes before beginning to differentiate during culture in retrorsine-exposed and PH-ized rats.

In conclusion, we demonstrated that annexin III mRNA was expressed in isolated small rat hepatocytes, but not in parenchymal hepatocytes, and that isolated small rat hepatocytes also express TAT and TO mRNA, two markers of highly differentiated hepatocyte phenotypes, indicating that the small hepatocytes have highly differentiated phenotypes. Since small hepatocytes can differentiate into parenchymal hepatocytes or biliary epithelial cells, as described in the introduction, such plasticity in phenotypes, including the dedifferentiation suggested by the results of the present study, may be regarded as one of the characteristic features of small hepatocytes that parenchymal hepatocytes do not share.

Acknowledgments This work was supported by grants for Health Science Research from the Japanese Ministry of Health, Labor and Welfare.

REFERENCES

1) Mitaka T., Sattler C. A., Sattler G. L., Sargent L. M., Pitot H. C., *Hepatology*, **13**, 21—30 (1991).
2) Mitaka T., Mikami M., Sattler G. L., Pitot H. C., Mochizuki Y., *Hepatology*, **16**, 440—447 (1992).
3) Tateno C., Yoshizato K., *Am. J. Pathol.*, **148**, 383—392 (1996).
4) Tateno C., Yoshizato K., *Am. J. Pathol.*, **149**, 1593—1605 (1996).
5) Karvountzis G. G., Redeker A. G., Peters R. L., *Gastroenterology*, **67**, 870—877 (1974).
6) Uchida T., Kronborg I., Peters R. L., *Hum. Pathol.*, **15**, 267—277 (1984).
7) Hino H., Tateno C., Sato H., Yamasaki C., Katayama S., Kohashi T., Aratani A., Asahara T., Dohi K., Yoshizato K., *Biochem. Biophys. Res. Commun.*, **256**, 184—191 (1999).
8) Niimi S., Oshizawa T., Yamaguchi T., Harashima M., Seki T., Ariga T., Kawanishi T., Hayakawa T., *Biochem. Biophys. Res. Commun.*, **300**, 770—774 (2003).
9) Tanaka K., Sato M., Tomita Y., Ichihara A., *J. Biochem.* (Tokyo), **84**, 937—946 (1978).
10) Tateno C., Takai-Kajihara K., Yamasaki C., Sato H., Yoshizato K., *Hepatology*, **31**, 65—74 (2000).
11) Gordon G. J., Coleman W. B., Grisham J. W., *Am. J. Pathol.*, **157**, 771—786 (2000).
12) Uno S., Nakamura M., Seki T., Ariga T., *Biochem. Biophys. Res. Commun.*, **239**, 123—128 (1997).
13) Pepinsky R. B., Tizard R., Mattaliano R. J., Sinclair L. K., Miller G. T., Browning J. L., Chow E. P., Burne C., Huang K. S., Pratt D., Wachter L., Hession C., Frey A. Z., Wallner B. P., *J. Biol. Chem.*, **263**, 10799—10811 (1988).
14) Masaki T., Tokuda M., Fujimura T., Ohnishi M., Tai Y., Miyamoto K., Itano T., Matsui H., Watanabe S., Sogawa K., Yamada T., Konishi R., Nishioka M., Hatase O., *Hepatology*, **20**, 425—435 (1994).
15) Della Gaspera B., Braut-Boucher F., Bomsel M., Chatelet F., Gugen-Guillouzo C., Font J., Weinman J., Weinman S., *Dev. Dyn.*, **222**, 206—217 (2001).
16) Sereni F., Kenney F. T., Kretchmer N., *J. Biol. Chem.*, **234**, 609—612 (1959).
17) Auerbach V. H., Waisman H. A., *J. Biol. Chem.*, **234**, 304—306 (1959).
18) Nemeth A. M., *J. Biol. Chem.*, **234**, 2921—2924 (1959).
19) Perry S. T., Rothrock R., Isham K. R., Lee K. L., Kenney F. T., *J. Cell. Biochem.*, **21**, 47—61 (1983).
20) Rothrock R., Lee K. L., Isham K. R., Johnson A. C., Kenney F. T., *Biochem. Biophys. Res. Commun.*, **144**, 1182—1187 (1987).
21) Killewich L. A., Feigelson P., *Proc. Natl. Acad. Sci. U.S.A.*, **74**, 5392—5396 (1977).
22) Nagao M., Nakamura T., Ichihara A., *Biochim. Biophys. Acta*, **867**, 179—186 (1986).
23) Shiojiri N., Lemire J. M., Fausto N., *Cancer Res.*, **51**, 2611—2620 (1991).
24) Miyazaki M., Akiyama I., Sakaguchi M., Nakashima E., Okada M., Kataoka K., Huh N. H., *Biochem. Biophys. Res. Commun.*, **298**, 24—30 (2002).
25) Meehan R. R., Barlow D. P., Hill R. E., Hogan B. L., Hastie N. D., *EMBO J.*, **3**, 1881—1885 (1984).
26) Gordon G. J., Coleman W. B., Hixson D. C., Grisham J. W., *Am. J. Pathol.*, **156**, 607—619 (2000).

Available online at www.sciencedirect.com
SCIENCE DIRECT®
Biomaterials 25 (2004) 1131–1140
Biomaterials
www.elsevier.com/locate/biomaterials

Preparation of lactose–silk fibroin conjugates and their application as a scaffold for hepatocyte attachment

Yohko Gotoh[a,*], Shingo Niimi[b], Takao Hayakawa[b], Tokuji Miyashita[c]

[a] *Insect Biomaterial and Technology Department, National Institute of Agrobiological Sciences, 1-2 Ohwashi, Tsukuba, Ibaraki 305-8634, Japan*
[b] *National Institute of Health Sciences, 1-18-1 Kamiyoga, Setagaya-ku, Tokyo 158-8501, Japan*
[c] *Institute of Multidisciplinary Research for Advanced Materials, Tohoku University, 2-1-1 Katahira, Aoba-ku, Sendai 980-8577, Japan*

Received 8 July 2003; accepted 30 July 2003

Abstract

We prepared glycoconjugates (Lac–CY–SF) by the homogeneous chemical modification of solubilized silk fibroin (SF) with lactose bearing the galactose residue using cyanuric chloride (CY) as a coupling spacer and examined the usefulness of their application as a scaffold for hepatocyte attachment. The covalent immobilization of lactose into SF was assessed by several criteria including ^{1}H-NMR measurements and reactions with lectins such as *Ricinus communis* agglutinin (RCA_{120}) and fluorescein isothiocyanate-labeled RCA_{120} (FITC-RCA_{120}). The ^{1}H-NMR spectrum of Lac–CY–SF showed new broad peaks attributed to methine and methylene protons of lactose, and by the integrated intensities of the peaks the weight ratio of lactose to SF in Lac–CY–SF was determined to be 0.20. Addition of RCA_{120} to Lac–CY–SF solution caused an increase in the turbidity of the Lac–CY–SF solution. Incubation of Lac–CY–SF films with FITC-RCA_{120} showed that the fluorescence emitted from the whole surface of Lac–CY–SF films. Furthermore, we examined the effect of the Lac–CY–SF conjugate-coating onto polystyrene culture dishes on the attachment of rat hepatocytes and their morphology. Attachment of hepatocytes onto the 0.1% (w/v) conjugate-coated dishes showed about an 8-fold increase as compared with that on uncoated dishes, being comparable to that on collagen-coated dishes, whereas the attachment on the SF-coated dishes was lower than that on uncoated dishes. Hepatocytes cultured onto the conjugate-coated dishes for 2.5 h showed smaller round-shaped morphology compared to those on collagen-coated dishes. After 2 days of culture in medium containing 100 nM insulin and 100 nM dexamethasone, hepatocytes on the conjugate-coated dishes formed monolayer islands with a slightly dispersed morphology, while hepatocytes cultured on collagen-coated dishes were uniformly spread flat. These results indicate that the Lac–CY–SF conjugates are useful as a scaffold for hepatocyte attachment, but the morphology of hepatocytes cultured on the conjugate-coated dishes is different from that on collagen-coated dishes.

Keywords: Silk fibroin; Lactose; Glycoconjugates; Galactose residues; Lectins; Hepatocytes

1. Introduction

Silk fibroin (SF) is a natural fibrous protein created by the *Bombyx mori* silkworm, and mainly consists of the Gly–Ala–Gly–Ala–Gly–Ser sequence having its native molecular weight of 370 kDa [1–3]. SF fiber has been used as a textile material for a long time. Recently, it has been found that SF aqueous solution can be easily reformed into gels [4,5], sponge [6], powder [7], and membranes [8,9], which have unique physicochemical properties [4–9] and biocompatibilities [10,11]. On the basis of these findings, SF has been reassessed as biotechnological and biomedical materials, for example, an oral dosage form [4,5], burn wound dressings [8], enzyme-immobilization matrices [9], and vascular prostheses [10].

Many current studies on SF aim at exploring SF-based scaffolds for tissue engineering [12–16]. Our previous studies indicated that attachment and growth of mouse fibroblast cells on SF-coated surfaces were comparable to those on collagen-coated surfaces [12,13]. Higuchi et al. investigated cell growth and the production of interferon-β for normal human skin cells cultured on both SF cast films and SF Langmuir–Blodgett (LB) films, and suggested that SF LB films are suitable for cell culture matrix for the purpose of the interferon-β production [14]. Moreover, osteoblast cell

*Corresponding author. Tel.: +81-29-838-6126; fax: +81-29-838-6028.
E-mail address: gotohy@affrc.go.jp (Y. Gotoh).

0142-9612/$ - see front matter © 2003 Elsevier Ltd. All rights reserved.
doi:10.1016/S0142-9612(03)00633-1

responses to SF-based scaffolds were investigated recently [15,16]. Sofia et al. demonstrated that SF cast films, the surface of which was covalently coupled with integrin recognition sequence (RGD), served as suitable bone-inducing matrices [15].

Recent studies on biological roles of oligosaccharides have revealed that many sugar residues in lipid molecules and proteins are quite effective in the recognition by animal lectins which are present at cell surfaces [17]. In particular, it is known that β-galactose residues are recognized by asialoglycoprotein receptors on the surfaces of hepatocytes [17,18] and promote hepatocyte attachment [19–24]. By making use of these sophisticated recognition mechanisms, synthetic polymers endowed with β-galactose residues as biological recognition signals have been developed as cell-specific culture substrata [19–24]. Therefore, it is considered that the β-galactose residues incorporated into SF may act as an efficient ligand for hepatocyte attachment to SF scaffolds.

We have been carrying out homogeneous chemical modification of amino acid residues of solubilized SF with oligosaccharides in aqueous solution using cyanuric chloride (CY) as a coupling spacer in order to alter SF properties and/or to functionalize SF [25,26]. In this paper, we prepared glycoconjugates (Lac–CY–SF) by the chemical modification of solubilized SF with lactose bearing the β-galactose residue using CY on the basis of these procedures and confirmed the covalent immobilization of lactose into SF by several criteria. Moreover, we examined the usefulness of the application of Lac–CY–SF as a scaffold for hepatocyte attachment.

2. Materials and methods

2.1. Materials

Lactose monohydrate and CY were purchased from Wako Pure Chemical Industries Ltd. (Osaka, Japan). All the other chemicals used for chemical modification were commercial reagent-grade products. *Ricinus communis* agglutinin (RCA_{120}) and fluorescein isothiocyanate-labeled RCA_{120} (FITC-RCA_{120}) were obtained from Sei-kagaku Co. (Tokyo, Japan). Phosphate buffer powder (1/15 mol/l, pH 7.0, Wako Pure Chemical Industries Ltd.) was used for the preparation of 150 mM NaCl–67 mM phosphate buffer of pH 7.0.

Williams' E (WE) medium was supplied by ICN Biomedicals Inc. (Costa Mesa, CA, USA). Aprotinin was obtained from Takara Biomedicals (Kyoto, Japan). Collagen type 1-AC for coating culture dishes was purchased from Koken Co. Ltd. (Tokyo, Japan). Bio-Rad protein assay kit (Bio-Rad Laboratories, Hercules, CA, USA) was used for measuring protein in hepatocyte lysates by the Bradford method with bovine serum albumin (BSA) as standard [27,28]. Other materials used for cell isolation and culture were as described by Tanaka et al. [29].

2.2. Preparation of the Lac–CY–SF conjugates

An aqueous solution of SF was prepared as described in our previous papers [12,13,25,26,30]. Briefly, cocoons from *B. mori* were degummed with boiling 0.5% (w/v) $NaHCO_3$ solution. The degummed SF fiber was dissolved in 9 M LiBr aqueous solution at 60°C. The dissolved solution was dialyzed against distilled water and then 1–2% (w/v) SF solution was obtained. The LiBr-solubilized SF has a heterogeneous molecular weight in the range of 30 kDa to more than 200 kDa [30].

Lac–CY–SF conjugates were synthesized on the basis of the preparation of the glycoconjugates between SF and chitin oligosaccharides [25] or chitosan oligosaccharides [26] using CY as a coupling spacer. The first step was the preparation of CY-activated lactose (Lac–CY) by the reaction of lactose with equivalent molar quantity of CY. A solution of 58 mg lactose monohydrate in 4.5 ml distilled water was cooled in an ice bath. To the lactose solution 30 mg CY in 1.5 ml 1,4-dioxane was slowly added at 4°C and about pH 9 by adding 20%(w/v) solution of Na_2CO_3 over 15 min. Then, the Lac–CY modifier was prepared by further stirring of the mixture at 4°C and pH 9 for 2 h. The Lac–CY solution was used for the second step, i.e., the coupling of lactose into SF, without purification. To the Lac–CY solution, 3.45 ml of 17.5 mg/ml SF aqueous solution containing 60 mg SF was added. The mixture was then incubated at 37°C and pH 8–9 for 3 h to make SF react with Lac–CY modifier.

The resulting mixture was neutralized by the addition of 1 N HCl to stop the reaction. The neutralized solution was dialyzed against distilled water using a Spectra/Por dialysis membrane (molecular weight cutoff of 12,000–14,000, Spectrum Laboratories, Inc., Rancho Dominguez, CA, USA) at 4°C overnight to remove unreacted reagents from the Lac–CY–SF product. The dialyzed solution was concentrated to about 4 ml using ultrafiltration with a Molecut-L TK-kit (Nihon Millipore Ltd., Tokyo, Japan). Although most of the unreacted reagents were considered to be removed by dialysis and ultrafiltration, further complete purification was carried out by gel filtration as described below.

The concentrated solution was applied to a column of Sephadex G50 (Amersham Pharmacia Biotech, Uppsala, Sweden) (ID 1.6 × 35 cm) preequilibrated with 2 M Urea–0.02 M Tris HCl (pH 8.0) and eluted with the same buffer at a flow rate of 0.46 ml/min. Fractions of 2.3 ml of the eluate were collected, and the protein content of each fraction was estimated by measuring the absorbance at 280 nm. Fractions corresponding to protein

peak were combined, and dialyzed thoroughly against distilled water at 4°C for a few days. The dialyzed solution was concentrated by ultrafiltration as described above. The obtained Lac–CY–SF solution (about 2% (w/v)) was cast onto polyethylene film and dried at ambient relative humidity at room temperature [8,25,26]. The prepared Lac–CY–SF films were further dried in a desiccator containing P_2O_5 for several days and 72 mg of the Lac–CY–SF product was obtained.

2.3. ^{1}H-NMR measurements

^{1}H-NMR spectra were recorded in D_2O at 300 MHz with a Varian 300BB NMR spectrometer and 3-(trimethylsilyl)-1-propanesulfonic acid sodium salt (DSS) was used as an internal standard. The samples of Lac–CY–SF, SF, and a mixture consisting of SF and lactose monohydrate (the weigh ratio of lactose monohydrate to SF was 0.29) were prepared by dissolving Lac–CY–SF films or SF films, which were obtained in a similar manner to that of Lac–CY–SF films, in D_2O, respectively. The ^{1}H-NMR spectra were measured at a concentration of 1–2% (w/v).

2.4. Recognition of the galactose residues in Lac–CY–SF by lectins

The lectin-induced agglutination of Lac–CY–SF was measured by the increase in absorbance at 350 nm at 25°C using a JASCO V-550 UV/vis spectrophotometer [31,32]. In both sample and reference cuvettes was placed 500 μl of 100 μg/ml Lac–CY–SF solution in 150 mM NaCl–67 mM phosphate buffer of pH 7.0, and a base line was recorded. Then, 50 μl of 2.6 mg/ml RCA_{120} solution in phosphate buffered saline (PBS) was added to the sample cuvette and quickly mixed. Agglutination of Lac–CY–SF was estimated by the time-dependent increase in absorbance at 350 nm. The reversibility of the agglutination was assessed by addition of 20 μl of 10 mg/ml free lactose solution in 150 mM NaCl–67 mM phosphate buffer (pH 7.0) [31,32]. A control experiment was carried out in which the Lac–CY–SF solution was replaced by 4 mg/ml SF solution in 150 mM NaCl–67 mM phosphate buffer (pH 7.0).

Water-insoluble films of Lac–CY–SF and SF were prepared by immersing each cast film into 10%(v/v) H_2O–90% (v/v) methanol solution for 1 h and being dried at room temperature [8,9,26]. A commercial solution of FITC-RCA_{120} in 50 mM Tris HCl (pH 7.4) was diluted to 0.53 mg/ml with 150 mM NaCl–67 mM phosphate buffer (pH 7.0). The insoluble films of Lac–CY–SF and SF were placed in 0.53 mg/ml FITC-RCA_{120} solution at room temperature for 30 min [33]. The films were washed 3 times with 150 mM NaCl–76 mM phosphate buffer (pH 7.0) and stored in the same buffer at 4°C until the observation by fluorescence microscope. Aggregation of FITC-RCA_{120} on the surface of Lac–CY–SF films was assessed using fluorescence microscope (Olympus IX-FLA) [33].

2.5. Hepatocyte attachment

Hepatocytes were isolated from the livers of 7-week-old male Wistar rats (180–200 g) by the modified collagenase perfusion technique of Seglen [34]. Isolated hepatocytes with higher than 85% viability as judged by trypan blue dye exclusion were used. The basal medium used was WE medium containing 30 μg/ml kanamycin and 1 μg/ml aprotinin. The cells were suspended at 1.96×10^5 cell/ml in the basal medium supplemented with 1 nM insulin and 1 nM dexamethasone. Other culture conditions were as reported previously [35].

Sample-coated dishes were prepared as follows. Aqueous sample solutions of Lac–CY–SF (1%(w/v), 0.1%(w/v), and 0.01%(w/v)), SF (1%(w/v), 0.1%(w/v), and 0.01%(w/v)), and SF–lactose mixture (1%(w/v) SF + 0.3%(w/v) lactose, 0.1%(w/v) SF + 0.03%(w/v) lactose, and 0.01%(w/v) SF + 0.003%(w/v) lactose) were sterilized by filtration using Millex-HV syringe-driven filter unit (pore size 0.45 μm, Nihon Millipore Ltd., Tokyo, Japan), respectively. An aliquot (0.10 ml) of the filtrate was placed in each well (11.2-mm-diameter dish) of polystyrene flat-bottomed 48-well plates for tissue culture (Iwaki Scitech Division, Asahi Techno Glass, Tokyo, Japan) at room temperature for 1 h to permit the sample to be absorbed on the surface of the dish. The solution was then removed and each well was rinsed with Dulbecco's phosphate buffered saline (without calcium chloride and magnesium chloride) (D-PBS(−)) to remove non-absorbed samples. Sample-coated dishes were stored in D-PBS(−) until use. As a positive control, collagen-coated dishes were prepared by the same procedure using 0.03% (w/v) collagen solution.

An aliquot (0.277 ml) of the hepatocyte suspensions (5.5×10^4 cells/cm^2) was seeded onto a sample-coated culture dish and cultured in a humidified chamber at 37°C under 5% CO_2 and 30% O_2 in air. After 2.5 h, non-adherent cells and the culture medium were removed and the attached cells was rinsed twice with D-PBS(−). The cells were lysed in 0.25 ml of 1 N NaOH at 37°C for 1 h. After centrifugation (12,000 rpm, 10 min), the protein amount of supernatant was determined by the Bradford method with BSA as standard [27,28]. Cell attachment degree of each sample was defined as a ratio of the protein amount derived from the cells on the sample to that on control collagen. All of the values given are the means of three independent measurements.

2.6. Morphological observations

Polystyrene 12-well plates (22.1-mm-diameter dish, Iwaki Scitech Division, Asahi Glass, Tokyo, Japan) were coated with 0.1% (w/v) Lac–CY–SF solutions and collagen solution in the manner shown above. The isolated hepatocytes were inoculated at a density of 6×10^4 cells/cm^2 in 0.7 ml of the basal medium containing 1 nM insulin and 1 nM dexamethasone. They were allowed to attach for 2.5 h as mentioned above. After 2.5 h of culture, the non-adherent cells were removed and the medium was replaced by 0.7 ml of hormone-defined WE medium, which consisted of the basal medium supplemented with 100 nM insulin and 100 nM dexamethasone. Subsequent cultivation was carried out, and the medium was exchanged every 24 h. Cell morphologies after 2.5 h and 2 days (2.5 h + 48 h) of culture were observed by phase-contrast microscope (Nikon DIAPHOT TMD). All experiments were performed twice, and the same tendency in the results was confirmed.

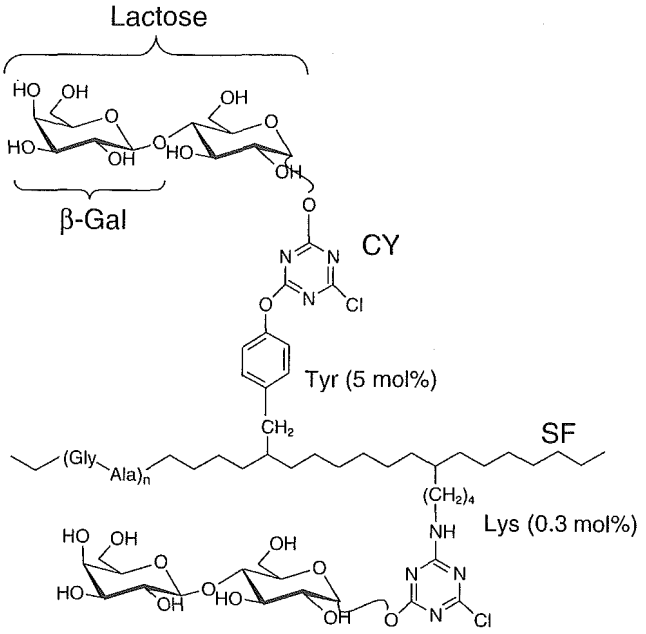

Fig. 2. Chemical structure of conjugates (Lac–CY–SF) consisting of silk fibroin (SF) and lactose.

3. Results

3.1. Preparation of the Lac–CY–SF conjugates

As shown in the reaction scheme of Fig. 1, oligosaccharides were covalently coupled with SF through CY as a spacer. It was clarified that the oligosaccharide–CY modifier was synthesized by the reaction of the amino group and/or the terminal anomeric hydroxyl group in oligosaccharides with a chlorine atom of CY, and then a second chlorine atom of the oligosaccharide–CY modifier reacted with the phenolic hydroxyl group of the tyrosine residue and ε-amino group of the lysine residue in SF [25,26]. Therefore, chemical structure of the Lac–CY–SF conjugates, which consists of SF and lactose bearing only anomeric hydroxyl group as a reaction site, is estimated as shown in Fig. 2.

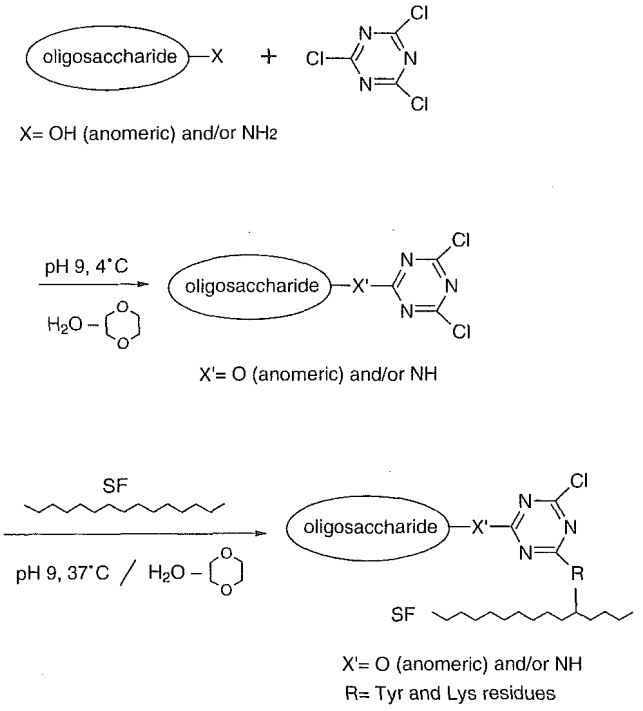

Fig. 1. Chemical modification of silk fibroin (SF) with cyanuric chloride (CY)-activated oligosaccharides.

The ^{1}H-NMR spectra of SF, a mixture of SF and lactose, and Lac–CY–SF are shown in Fig. 3. The spectrum of Lac–CY–SF showed new broad peaks attributed to methine and methylene protons of lactose in the interval 3.4–3.7 ppm and at about 4.6 ppm in addition to the SF peaks. This indicates the successful introduction of lactose into SF by chemical modification. Moreover, in the spectrum of Lac–CY–SF, a broad peak appeared in the interval 6.96–7.4 ppm overlapping with the peak of the aromatic protons of the phenylalanine residue while original peaks at 6.79 and 7.07 ppm attributed to the aromatic protons of the tyrosine residue in SF [25,26] disappeared. This downfield shift was caused by the deshielding of the triazine ring of CY [25,26] and supported the fact that the phenolic hydroxyl group of the tyrosine residue in SF reacted with the Lac–CY modifier.

Chemical composition of Lac–CY–SF was determined by comparing the integral values of the resonance peaks of Lac–CY–SF, SF, and a mixture of SF and lactose of known composition. In each spectrum, the integral value of the β-methyl protons of the alanine residue in SF at 1.38 ppm, which was not modified with

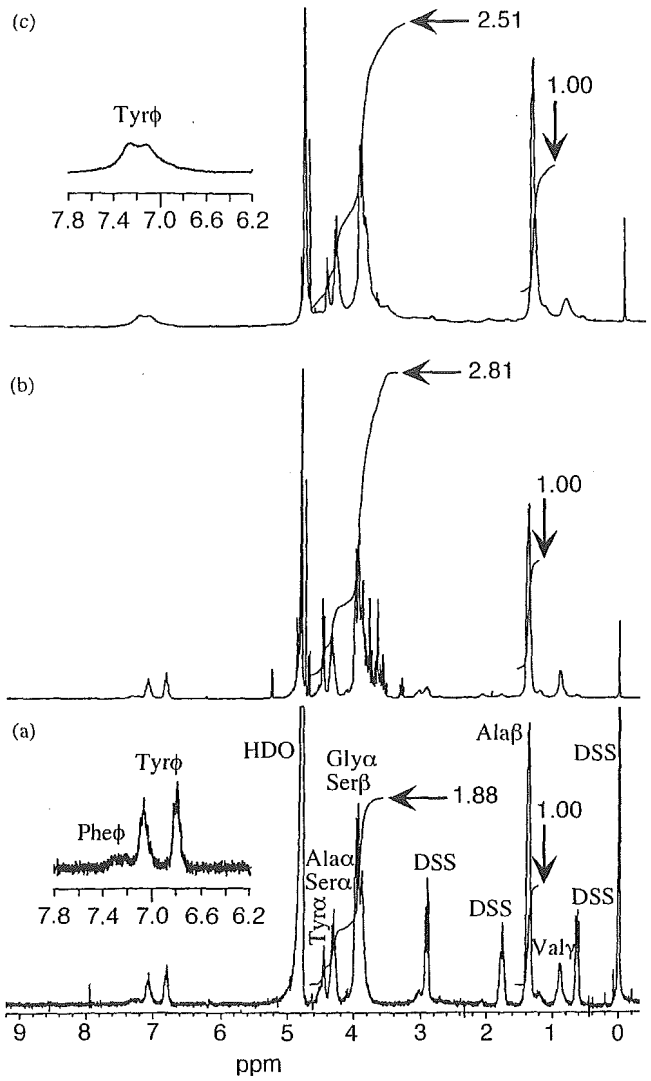

Fig. 3. ^{1}H-NMR spectra of SF (a), a mixture of SF and lactose with a lactose/SF weight ratio of 0.29 (b), and Lac–CY–SF (c) in D_2O.

Lac–CY, was used as an integration reference. The integral value of the peaks in the interval 3.4–4.6 ppm was measured for each sample (Fig. 3). The spectrum of SF showed that the integral value of the peaks in the interval 3.6–4.6 ppm was 1.88 (Fig. 3(a)). In the spectrum of a mixture of SF and lactose (the weight ratio of lactose to SF was 0.29), the integral value of the peaks attributed to SF and lactose in the interval 3.4–4.6 ppm was 2.81 (Fig. 3(b)). These results suggested that the integral value of the peaks attributed to lactose in the interval 3.4–4.6 ppm was 0.98 (=2.81–1.88) in the spectrum of the mixture. In the spectrum of Lac–CY–SF, since the integral value of the peaks attributed to SF and lactose in the interval 3.4–4.6 ppm was 2.51 (Fig. 3(c)), the integral value of the peaks attributed to lactose in the interval 3.4–4.6 ppm was 0.63 (=2.51–1.88). Therefore, it was calculated that the value of the lactose content in Lac–CY–SF was 68% (=0.68/0.93) of that in the mixture of SF and lactose. This means that the weight ratio of lactose to SF in Lac–CY–SF was 0.20 (=0.29 × 0.68). From 60 mg SF starting material, 72 mg Lac–CY–SF product was obtained. When the weight occupied by the triazine ring (C_3N_3Cl=113.5) was disregarded in the calculation, the weight ratio of lactose to SF in the conjugates was roughly calculated to be 0.20 (=(72–60)/60). This value is consistent with the value obtained by the integration of the peaks in NMR spectra.

It was clarified that the reaction sites of SF with oligosaccharide–CY modifier are the tyrosine and lysine residues, the content of which are 5.2 and 0.3 mol%, respectively [25,26]. The average molecular weight of the amino acid unit constituting SF is 75 [25,26], and the molecular weight of lactose monohydrate is 360. If all of the tyrosine and lysine residues in SF react with the modifier and the weight of SF in the Lac–CY–SF conjugates is assumed to be unity, the weight ratio of lactose to SF in the conjugates is calculated to be 0.26 (=(1/75) × 0.055 × 360). Although this expected value is somewhat larger than the experimental values obtained from the integrated intensities of NMR peaks and from the yield of the product, the expected value does not significantly deviate from the experimental values.

3.2. *Recognition of the galactose residues in Lac–CY–SF by lectins*

We studied interactions between Lac–CY–SF and lectins to confirm the covalent immobilization of lactose bearing the β-galactose residues into SF. Fig. 4 shows the typical turbidity changes observed by the addition of RCA_{120} lectins to Lac–CY–SF or SF solution. Since the turbidity increase was not observed for the SF solution as shown in Fig. 4, there was no nonspecific lectin-mediated aggregation of SF. In contrast, the turbidity of the Lac–CY–SF solution rapidly increased after the addition of RCA_{120} and the aggregation of Lac–CY–SF was observed (Fig. 4). This lectin-induced aggregation

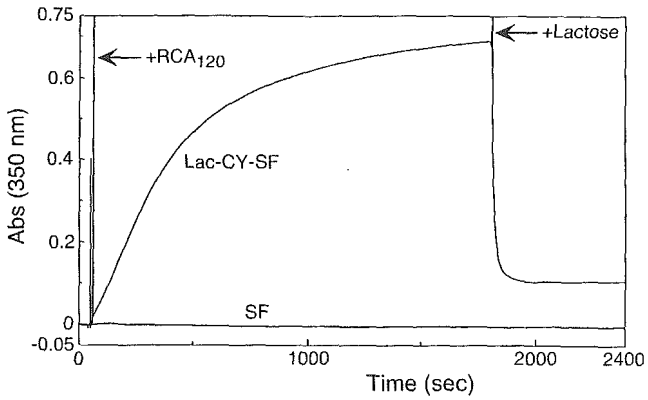

Fig. 4. Time course of turbidity changes of Lac–CY–SF and SF at 350 nm after addition of RCA_{120} lectins.

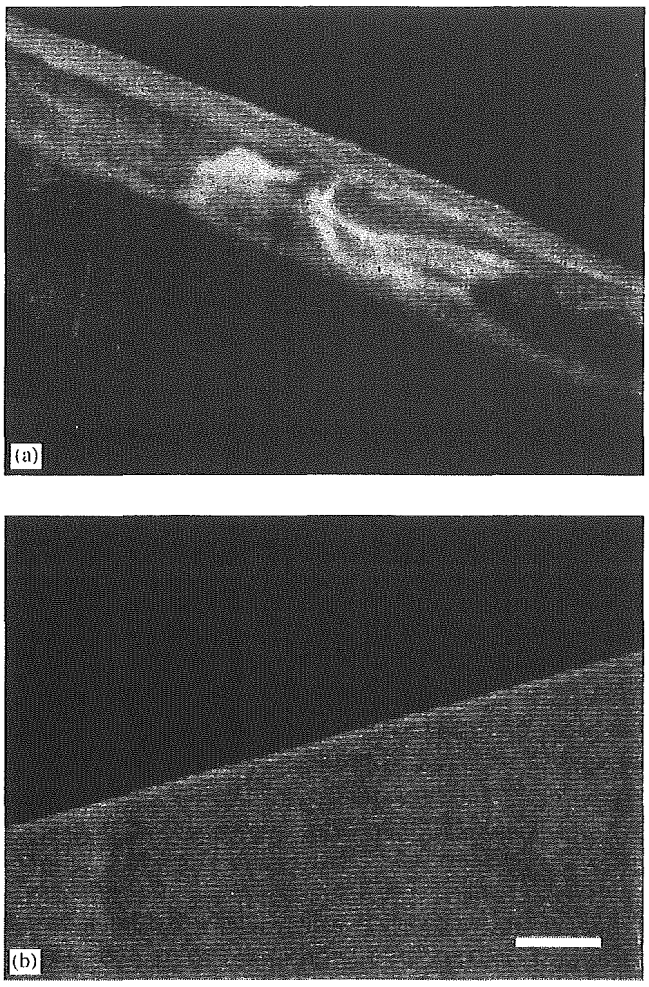

Fig. 5. Fluorescence images of cast films of Lac–CY–SF (a) and SF (b) after immersion into FITC-RCA_{120} solution. Scale bar indicates 100 μm.

was promptly reversed by the addition of excess free lactose (Fig. 4).

The fluorescence microscopic images of Lac–CY–SF and SF films after incubation with FITC-RCA_{120} are shown in Fig. 5. Upon irradiating the films with G-excitation light, yellow fluorescence was emitted from the whole surface of Lac–CY–SF films while fluorescence was not observed for SF films.

3.3. *Attachment of hepatocytes onto the Lac–CY–SF conjugate-coated dishes*

Attachment of hepatocytes onto the sample-coated dishes was examined after the cultivation in serum-free WE medium for 2.5 h as shown in Fig. 6. The attachment on SF-coated dishes was lower than that on uncoated polystyrene dishes whatever the SF concentration. The attachment on the dishes coated with the solutions of a mixture of SF and lactose was very low and similar to that on SF-coated dishes whatever the concentration (Fig. 6).

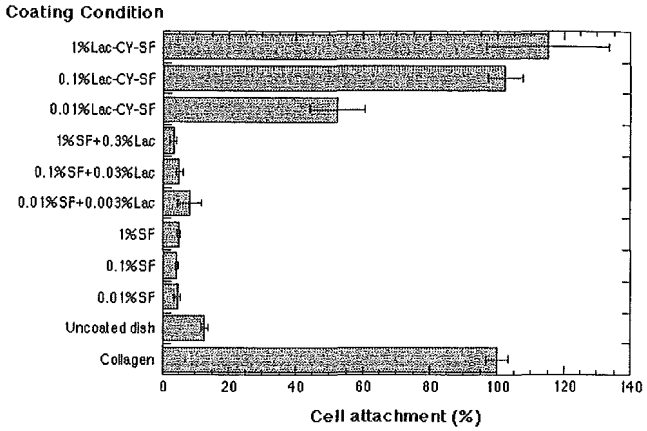

Fig. 6. Attachment of hepatocytes onto the dishes coated with solutions of SF, a mixture of SF and lactose (SF + Lac), and Lac–CY–SF after the cultivation in WE medium for 2.5 h.

In contrast, noticeable increase of cell attachment was found for the Lac–CY–SF conjugate-coated dishes. The attachment on the dishes coated with 0.01%(w/v) solution of Lac–CY–SF was considerably higher than that on uncoated polystyrene dishes but was lower than that on collagen-coated dishes. Moreover, the attachment on the dishes coated with 0.1%(w/v) and 1%(w/v) solutions of Lac–CY–SF showed an 8–9-fold increase as compared with that on uncoated polystyrene dishes, being comparable to that on collagen-coated dishes.

3.4. *Morphologies of hepatocytes*

The morphologies of hepatocytes cultured on the dishes coated with 0.1%(w/v) Lac–CY–SF for 2.5 h and 2 days were compared with those on collagen-coated dishes (Figs. 7 and 8). The morphologies of attached hepatocytes on the dishes coated with 0.1% (w/v) Lac–CY–SF after 2.5 h were small and round, being obviously different from large ones on collagen-coated dishes (Fig. 7). Furthermore, when hepatocytes cultured on the Lac–CY–SF conjugate-coated dishes for 2 days, the attached cells migrated to assemble with each other and formed monolayer islands with a slightly dispersed morphology, being obviously different from the very flat and completely dispersed ones on collagen-coated dishes (Fig. 8).

4. Discussion

We prepared glycoconjugates Lac–CY–SF by the homogeneous chemical modification of solubilized SF with lactose bearing the β-galactose residue using CY as a coupling spacer. The covalent immobilization of lactose into SF was confirmed by criteria including ^{1}H-NMR measurements and the reactions with lectins. The ^{1}H-NMR spectrum of Lac–CY–SF showed new

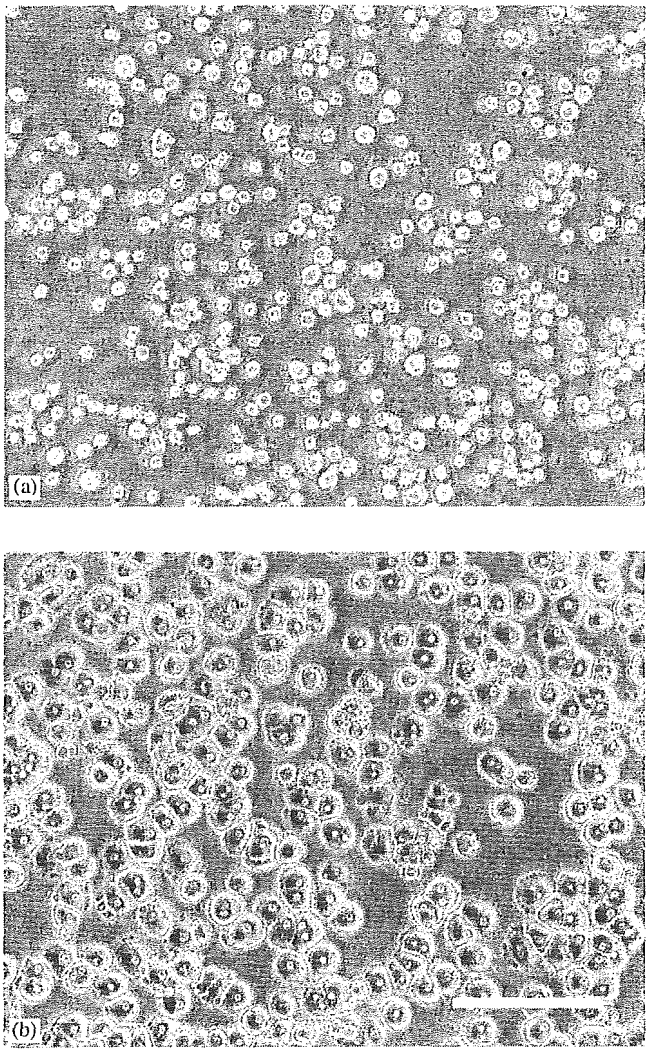

Fig. 7. Phase-contrast micrographs of hepatocytes on dishes coated with 0.1%(w/v) Lac–CY–SF (a) and collagen (b) after the cultivation for 2.5 h. Scale bar indicates 50 μm.

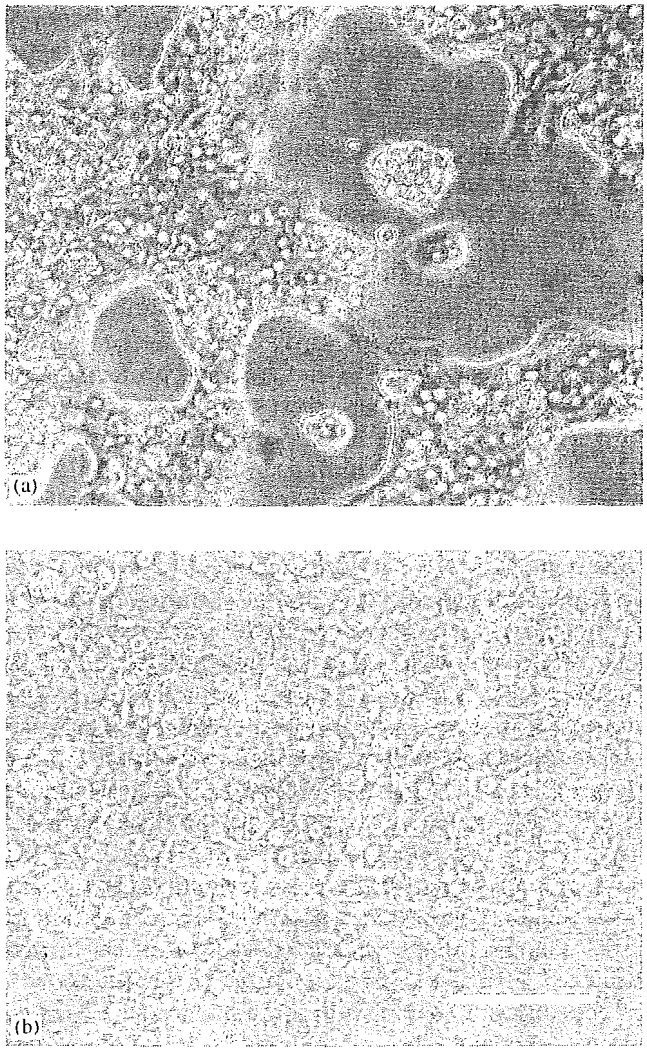

Fig. 8. Phase-contrast micrographs of hepatocytes on dishes coated with 0.1%(w/v) Lac–CY–SF (a) and collagen (b) after the cultivation for 2 days. Hepatocytes were cultured in hormone-defined WE medium containing insulin and dexamethasone. Scale bar indicates 50 μm.

broad peaks attributed to the methine and methylene protons of lactose, and by the integrated intensities of the peaks the weight ratio of lactose to SF was determined to be 0.20 (Fig. 3). Incubation of Lac–CY–SF solution with RCA_{120} lectins resulted in the increase of turbidity (Fig. 4) attributed to the specific recognition of the galactose residue in Lac–CY–SF by RCA_{120} lectins and subsequent aggregation of Lac–CY–SF mediated by cross-linking with lectin molecules [31,32]. The reversibility of the aggregation by the addition of free lactose provided evidence for the dissociation of the Lac–CY–SF conjugates cross-linked with RAC_{120} lectins which present a greater selectivity for free lactose [31,32]. These results suggest that the prepared Lac–CY–SF was not a mixture of SF and lactose but a galactose-immobilized polymer which induced the aggregation with lectins. Moreover, the fluorescence image of Lac–CY–SF films after incubation with FITC-RCA_{120} lectins depicted the fixation of FITC-RCA_{120} lectins onto the whole surface of Lac–CY–SF films (Fig. 5), indicating the existing of the galactose residue in the whole surface of Lac–CY–SF films. Therefore, it was suggested that although most of the hydrophilic lactose moieties were coupled to the tyrosine residues which are homogeneously present in relatively hydrophobic SF proteins [3], the galactose residues of Lac–CY–SF films were not buried in SF moieties but well exposed to be recognized by lectins in an aqueous medium.

As it was demonstrated that the galactose residues in the Lac–CY–SF conjugates were valid as recognition ligands in solid substrates, the effect of the galactose residues on the attachment of hepatocytes was examined by using the Lac–CY–SF conjugate-coated dishes and serum-free WE medium. From the results for hepatocyte attachment on SF-coated dishes, shown in Fig. 6, it was found that although the coating with 0.01%(w/v) SF solution was sufficient to fix SF proteins by adsorption

on the surface of polystyrene culture dishes, SF proteins have an inhibitory effect on the attachment of hepatocytes. In contrast to SF-coating, the Lac–CY–SF conjugate-coating onto polystyrene dishes promoted cell attachment. The amounts of cells attached on the dishes coated with 0.1%(w/v) and 1%(w/v) solutions of Lac–CY–SF were comparable to those on collagen-coated dishes (Fig. 6). The enhancement of cell attachment was not observed in the dishes coated with a mixture of SF and lactose (Fig. 6). Thus, it was evident that free lactose molecules were not adsorbed to the surface of culture dishes while SF proteins were adsorbed. These results suggest that Lac–CY–SF was properly adsorbed on the surface of dishes via interaction of the SF moiety with the surface and that the cell efficiently attached to the surface via interaction of the lactose moiety with the cells. Our present results are consistent with the previous findings of the enhanced attachment of hepatocytes onto the surfaces coated with lactose-carrying polystyrene (PVLA) and other polymers endowed with galactose moieties [19–24]. The enhancement of cell attachment in these studies was shown to be due to the binding of galactose residues with asialoglycoprotein receptors expressed on the cell surface [19–24]. As the expression of a galactose-specific lectin was limited to some type of cells such as hepatocytes and macrophages [17,18,31,32], Lac–CY–SF may be also useful for the selection of hepatocytes from isolated liver cells containing other population of cells. The usefulness of Lac–CY–SF can be further indicated by the results that the cell attached on SF-coated dishes was even lower than that on uncoated dishes, showing the inhibition of the non-specific attachment of the cells by SF. This is the first report indicating that the SF protein endowed with the galactose moiety is a promising biopolymer as a scaffold for hepatocyte attachment.

Since we found that the surfaces coated with the Lac–CY–SF solutions, the concentrations of which were higher than 0.1%(w/v), were effective for hepatocyte attachment, we studied the morphologies of hepatocytes attached on the dishes coated with 0.1%(w/v) Lac–CY–SF solution. We observed that round-shaped hepatocytes cultured on the conjugate-coated dishes for 2.5 h were smaller than round ones on collagen-coated dishes (Fig. 7). It was also reported that round-shaped hepatocytes on the PVLA-coated dishes were small compared to those on collagen-coated dishes after cultivation for 3 h [36]. During 2 days of culture, hepatocytes on collagen-coated dishes spread out and formed a confluent monolayer (Fig. 8(b)). On the conjugate-coated dishes, hepatocytes cultured in hormone-defined medium for 2 days showed a less flattened and less dispersed shape than did those on collagen-coated dishes (Fig. 8(a)). Interestingly, it is known that a liver-specific function, e.g., albumin secretion, of round hepatocytes is higher than that of flat hepatocytes [37,38]. It was also reported that round hepatocytes on PVLA-coated dishes expressed higher levels of liver-specific genes than did flat hepatocytes on collagen-coated dishes [38,39]. Thus, it is likely that liver-specific functions of hepatocytes cultured onto the Lac–CY–SF conjugate-coated dishes may become higher than those of hepatocytes on collagen-coated dishes. Further study is required to ascertain this possibility.

In addition to the monolayer culture, evidence suggests that Lac–CY–SF may be useful for forming multilayer aggregates (spheroids) of hepatocytes and as the three-dimensional scaffolds for hepatocytes culture as described below. The spheroids are formed on the surfaces coated with PVLA and other synthetic and natural polymers endowed with galactose moieties in the presence of epidermal growth factor and insulin during culture and maintain the high level of liver-specific functions [23,24,40]. Therefore, such spheroids may be formed in the similar culture conditions by using Lac–CY–SF instead of the polymers endowed with galactose moieties. Current research on an artificial liver support system is being focused on three-dimensional substrate configurations for hepatocyte culture. In this respect, it is noteworthy that Lac–CY–SF can coat the surfaces of microcarriers and hollow fibers in the culture module such as a bioreactor. Moreover, we found that water-insoluble porous sponge-like scaffolds of Lac–CY–SF were fabricated by freeze-drying of an aqueous Lac–CY–SF solution according to the preparation of the porous SF materials [6], followed by immersion in methanol aqueous solutions (unpublished results). Therefore, Lac–CY–SF may be applied for three-dimensional scaffolds for hepatocyte culture.

5. Conclusions

We prepared new glycoconjugates Lac–CY–SF composed of SF and lactose bearing the galactose residue with a lactose/SF weight ratio of 0.20. The covalent immobilization of the galactose residue into SF was confirmed by the criteria including ^{1}H-NMR measurements and the reactions with RCA_{120} and with FITC-RCA_{120}. Although hepatocyte attachment on SF-coated dishes was lower than that on uncoated polystyrene dishes, the attachment on the dishes coated with 0.1%(w/v) and 1%(w/v) solutions of Lac–CY–SF was comparable to that on collagen-coated dishes. After 2 days of culture, hepatocytes on the conjugate-coated dishes showed a small amount of dispersion compared to those on collagen-coated dishes. These results support the concept that the Lac–CY–SF glycoconjugates can serve as a scaffold for hepatocyte attachment.

Acknowledgements

The authors wish to thank Dr. Teruhiko Baba (National Institute of Advanced Industrial Science and Technology) for his helpful comments on the manuscript, and Dr. Makoto Ide (Department of Material Systems Engineering and Life Science, Toyama University) for useful advice in carrying out the lectin-induced aggregation. The authors are also indebted to Dr. Yasushi Tamada (National Institute of Agrobiological Sciences) for obtaining the fluorescence images and Ms. Mami Nabeshima (National Institute of Advanced Industrial Science and Technology) for measuring the NMR spectra.

References

[1] Kaplan D, Adams WW, Farmer B, Viney C. Silk polymers. Materials science and biotechnology (American Chemical Society Symposium Series 544). Washington, DC: American Chemical Society; 1994.
[2] Kaplan DL, Mello CM, Arcidiacono S, Fossey S, Senecal K, Muller W. Silk. In: McGrath K, Kaplan D, editors. Protein-based materials. Boston: Birkhauser; 1997. p. 103–31.
[3] Zhou C-Z, Confalonieri F, Medina N, Zivanovic Y, Esnault C, Yang T, Jacquet M, Janin J, Duguet M, Perasso R, Li Z-G. Fine organization of *Bombyx mori* fibroin heavy chain gene. Nucl Acids Res 2000;28:2413–9.
[4] Hanawa T, Watanabe A, Tsuchiya T, Ikoma R, Hidaka M, Sugihara M. New oral dosage form for elderly patients: preparation and characterization of silk fibroin gel. Chem Pharm Bull 1995;43:284–8.
[5] Hanawa T, Watanabe A, Tsuchiya T, Ikoma R, Hidaka M, Sugihara M. New oral dosage form for elderly patients. II. Release behavior of benfotiamine from silk fibroin gel. Chem Pharm Bull 1995;43:872–6.
[6] Li M, Lu S, Wu Z, Yan H, Mo J, Wang L. Study on porous silk fibroin materials. I. Fine structure of freeze dried silk fibroin. J Appl Polym Sci 2001;79:2185–91.
[7] Akiyama D, Kitahara Y, Xuan L, Murakami M, Arai M, Hirabayashi K. Preparation of silk powder and the properties of the molded materials. Sen-i Gakkaishi (J Soc Fiber Sci Tec, Jpn) 1991;47:339–44.
[8] Minoura N, Tsukada M, Nagura M. Physico-chemical properties of silk fibroin membrane as a biomaterial. Biomaterials 1990;11:430–4.
[9] Demura M, Asakura T, Kuroo T. Immobilization of biocatalysts with *Bombyx mori* silk fibroin by several kinds of physical treatment and its application to glucose sensors. Biosensors 1989;4:361–72.
[10] Sakabe H, Ito H, Miyamoto T, Noishiki Y, Ha WS. In vivo blood compatibility of regenerated silk fibroin. Sen-i Gakkaishi 1989;45:487–90.
[11] Santin M, Motta A, Freddi G, Cannas M. In vitro evaluation of the inflammatory potential of the silk fibroin. J Biomed Mater Res 1999;46:382–9.
[12] Minoura N, Aiba S-I, Higuchi M, Gotoh Y, Tsukada M, Imai Y. Attachment and growth of fibroblast cells on silk fibroin. Biochem Biophys Res Commun 1995;208:511–6.
[13] Gotoh Y, Tsukada M, Minoura N. Effect of the chemical modification of the arginyl residue in *Bombyx mori* silk fibroin on the attachment and growth of fibroblast cells. J Biomed Mater Res 1998;39:351–7.
[14] Higuchi A, Yoshida M, Ohno T, Asakura T, Hara M. Production of interferon-β in a culture of fibroblast cells on some polymeric films. Cytotechnology 2000;34:165–73.
[15] Sofia S, McCarthy MB, Gronowicz G, Kaplan DL. Functionalized silk-based biomaterials for bone formation. J Biomed Mater Res 2001;54:139–48.
[16] Cai K, Yao K, Lin S, Yang Z, Li X, Xie H, Qing T, Gao L. Poly(D, L-lactic acid) surfaces modified by silk fibroin: effects on the culture of osteoblast in vitro. Biomaterials 2002;23:1153–60.
[17] Varki A. Biological roles of oligosaccharides: all of the theories are correct. Glycobiology 1993;3:97–130.
[18] Ashwell G, Harford J. Carbohydrate-specific receptors of the liver. Ann Rev Biochem 1982;51:531–54.
[19] Weigel PH, Schnaar RL, Kuhlenschmidt MS, Schmell E, Lee RT, Lee YC, Roseman S. Adhesion of hepatocytes to immobilized sugars. J Biol Chem 1979;254:10830–8.
[20] Oka JA, Weigel PH. Binding and spreading of hepatocytes on synthetic galactose culture surfaces occur as distinct and separable threshold responses. J Cell Biol 1986;103:1055–60.
[21] Kobayashi A, Akaike T, Kobayashi K, Sumitomo H. Enhanced adhesion and survival efficiency of liver cells in culture dished coated with a lactose-carrying styrene homopolymer. Makromol Chem Rapid Commun 1986;7:645–50.
[22] Kobayashi A, Goto M, Kobayashi K, Akaike T. Receptor-mediated regulation of differentiation and proliferation of hepatocytes by synthetic polymer model of asialoglycoprotein. J Biomater Sci Polym Edn 1994;6:325–42.
[23] Yang J, Goto M, Ise H, Cho C-S, Akaike T. Galactosylated alginate as a scaffold for hepatocytes entrapment. Biomaterials 2002;23:471–9.
[24] Yoon JJ, Nam YS, Kim JH, Park TG. Surface immobilization of galactose onto aliphatic biodegradable polymers for hepatocyte culture. Biotechnol Bioeng 2002;78:1–10.
[25] Gotoh Y, Tsukada M, Aiba S-I, Minoura N. Chemical modification of silk fibroin with *N*-acetyl-chito-oligosaccharides. Int J Biol Macromol 1996;18:19–26.
[26] Gotoh Y, Minoura N, Miyashita T. Preparation and characterization of conjugates of silk fibroin and chitooligosaccharides. Colloid Polym Sci 2002;280:562–8.
[27] Bradford MM. A rapid and sensitive method for the quantitation of microgram quantities of protein utilizing the principle of protein-dye binding. Anal Biochem 1976;72:248–54.
[28] Gogstad GO, Krutnes M-B. Measurement of protein in cell suspensions using the coomassie brilliant blue dye-binding assay. Anal Biochem 1982;126:355–9.
[29] Tanaka K, Sato M, Tomita Y, Ichihara A. Biochemical studies on liver functions in primary cultured hepatocytes of adult rats. J Biochem 1978;84:937–46.
[30] Tsukada M, Gotoh Y, Minoura N. Characterization of the regenerated silk fibroin from *Bombyx mori*. J Seric Sci Jpn 1990;59:325–30.
[31] Haensler J, Schuber F. Preparation of neo-galactosylated liposomes and their interaction with mouse peritoneal macrophages. Biochim Biophys Acta 1988;946:95–105.
[32] Kawaguchi T, Tagawa K, Senda F, Matsunaga T, Kitano H. Recognition of amphiphiles with many pendent galactose residues by *Ricinus communis* agglutinin. J Colloid Interface Sci 1999;210:290–5.
[33] Nishikawa T, Nishida J, Ookura R, Nishimura S-I, Wada S, Karino T, Shimomura M. Honeycomb-patterned thin films of amphiphilic polymers as cell culture substrates. Mater Sci Eng C 1999;8-9:495–500.
[34] Seglen PO. Preparation of isolated rat liver cells. Methods Cell Biol 1976;13:23–83.

[35] Niimi S, Hayakawa T, Tanaka A. Hormonal regulation of growth hormone receptors in primary cultured rat hepatocytes. Endocrinology 1990;127:688–94.
[36] Watanabe Y, Ajioka I, Akaike T. Gene transfection of multicellular spheroid of hepatocytes on an artificial substrate. Cytotechnology 1998;26:65–78.
[37] Singhvi R, Kumar A, Lopez GP, Stephanopoulos GN, Wang DIC, Whitesides GM, Ingber DE. Engineering cell shape and function. Science 1994;264:696–8.
[38] Oda H. Extracellular matrix regulates hepatocyte gene expression and differentiation. Connect Tissue 1998;30:225–32.
[39] Matsushita N, Oda H, Kobayashi K, Akaike T, Yoshida A. Induction of cytochrome P-450s and expression of liver-specific genes in rat primary hepatocytes cultured on different extracellular matrices. Biosci Biotech Biochem 1994;58:1514–6.
[40] Tobe S, Takei Y, Kobayashi K, Akaike T. Tissue reconstruction in primary cultured rat hepatocytes on asialoglycoprotein model polymer. Artif Organs 1992;16:526–32.

Suppression of Proliferation of Poliovirus and Porcine Parvovirus by Novel Phenoxazines, 2-Amino-4,4α-dihydro-4α-7-dimethyl-3*H*-phenoxazine-3-one and 3-Amino-1,4α-dihydro-4α-8-dimethyl-2*H*-phenoxazine-2-one

Akiko IWATA,[a] Teruhide YAMAGUCHI,[a] Kouei SATO,[b] Noriko YOSHITAKE,[c] and Akio TOMODA*,[d]

[a] *Division of Cellular and Gene Therapy Products, National Institute of Health, Sciences; 1–18–1 Kamiyoga, Setagaya-ku, Tokyo 158–0098, Japan:* [b] *The Institute of Saitama Red Cross Cente; 8–3–41 Kamiochiai, Saitama, Saitama 338–0001, Japan:* [c] *Third Department of Internal Medicine, Tokyo Medical University; and* [d] *Department of Biochemistry and Intractable Immune System Disease Research Center, Tokyo Medical University; 6–1–1 Shinjuku, Tokyo 160–0022, Japan.*
Received October 7, 2004; accepted January 5, 2005

The present study aimed at investigating the antiviral effects of 2-amino-4,4α-dihydro-4α-7-dimethyl-3*H*-phenoxazine-3-one (Phx-1) and 3-amino-1,4α-dihydro-4α-8-dimethyl-2*H*-phenoxazine-2-one (Phx-2) on 6 representative viruses: poliovirus, porcine parvovirus, simian virus 40 (SV-40), herpes simplex virus-1 (HSV-1), Sindbis virus, and vesicular stomatitis virus (VSV). Phx-1 and Phx-2 suppressed the proliferation of poliovirus in Vero cells and that of porcine parvovirus in ESK cells at concentrations between 0.25 μg/ml and 2 μg/ml, when the cells were treated with Phx-1 and Phx-2 for 1 h and then inoculated with these viruses. The proliferation of the other viruses, SV-40, HSV-1, Sindbis virus, and VSV, in the host cells was not influenced by Phx-1 or Phx-2 at concentrations less than 20 μg/ml. The results suggest that Phx-1 and Phx-2 may be useful to prevent the proliferation of poliovirus and porcine parvovirus infection and may contribute to developing new antiviral drugs in future.

Key words phenoxazine; poliovirus; porcine parvovirus

The development of antiviral drugs has been undertaken in parallel with that of vaccines, so as to overcome viral infections. Vaccination has been adopted to prevent several viral infections due to poliovirus, poxvirus, influenza virus *etc.* However, the usefulness of the antiviral drugs discovered so far seems to be restricted by the adverse effects of the drugs and the appearance of drug-resistant viruses.[1,2]

On the other hand, Tomoda *et al.* found that relatively water-soluble phenoxazines were biosynthesized by the reaction of *o*-aminophenol and its derivatives with human and bovine hemoglobin.[3—5] Among these phenoxazines, 2-amino-4,4α-dihydro-4α-7-dimethyl-3*H*-phenoxazine-3-one (Phx-1) has been demonstrated to have anticancer activity.[6,7] It was also shown that Phx-1 exerts an immunosuppressive effect on the activated lymphocytes such as B cells and T cells[8,9] and the activated mast cells.[10] Therefore, it seems of interest to investigate the effects of water-soluble phenoxazines on the proliferation of viruses in the host cells. We briefly reported that the proliferation of poliovirus inoculated to Vero cells was inhibited by Phx-1.[11] This discovery prompted us to investigate the effects of water-soluble phenoxazines on various kinds of viruses, because there is a possibility that a new antiviral drug may be developed through such an investigation. The present manuscript deals with studies on the antiviral effects of Phx-1 and 2-amino-4,4α-dihydro-4α-7-dimethyl-3*H*-phenoxazine-3-one (Phx-2) on 6 representative viruses: poliovirus, porcine parvovirus, simian virus (SV-40), herpes simplex virus-1 (HSV-1), Sindbis virus, and vesicular stomatitis virus (VSV).

MATERIALS AND METHODS

Phx-1, Phx-2, Cells and Viruses Phx-1 and Phx-2 were prepared by reaction of bovine hemoglobin with 2-amino-5-methylphenol and 2-amino-4-methylphenol, respectively, as previously described.[4,5] The chemical structures of Phx-1 and Phx-2 are shown in Fig. 1. Phx-1 or Phx-2 was dissolved in dimethyl sulfoxide (DMSO) before use to reach a concentration of 20 mM, and then was diluted with α-minimum essential medium (α-MEM).

African green monkey kidney cells (Vero cells), were generously supplied by the Japanese Cancer Research Resources Bank (Tokyo, Japan). The ESK cells (embryonic swine kidney cells line)[12] were kindly donated by Dr. J. Koga (JCR Co., Japan).

Cells were maintained in α-MEM supplemented with 10% fetal calf serum (FCS, Sigma Co., Ltd., St. Louis, MO, U.S.A.), and 30 mg/l kanamycin sulfate RPMI 1640 medium containing 10% heat-inactivated FCS, at 37 °C under moisturized air containing 5% CO_2.

Poliovirus (strain Sabin 1) was also donated by Dr. Koga. Porcine parvovirus (strain 90HS), SV-40, Sindbis virus, and HSV-1 (strain F) were the generous donation of Dr. M. Kohase (National Institute of Infectious Diseases). VSV (strain NJ) was the gift of Dr. H. Kita (Suntory Center Institute, Japan).

The supernatants of Vero cells infected with poliovirus, HSV-1, Sindbis virus, and VSV were used as the virus samples. The supernatant of ESK cells infected with porcine parvovirus was used as the porcine parvovirus sample. CV-1 cells were infected with SV-40 virus, and then 5 d after infec-

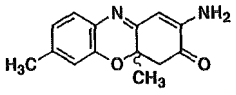

Phx-1

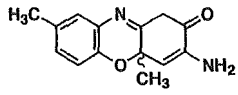

Phx-2

Fig. 1. Chemical Structures of Phx-1 and Phx-2

* To whom correspondence should be addressed. e-mail: tomoda@tokyo-med.ac.jp

Table 1. Effects of Phx-1 or Phx-2 on the Proliferation of Poliovirus Inoculated to Vero Cells at Different Concentrations of Phx-1 and Phx-2, Estimated by $TCID_{50}$[a)]

	Phx-1 (μg/ml)					Phx-2 (μg/ml)				
	0	0.25	0.55	1	2	0	0.25	0.5	1	2
$TCID_{50}$	62	32	32	16	17	63	63	63	63	14

a) $TCID_{50}$ was defined as dilution ratio of the virus to generate 50% disruption of the cells.

tion, the supernatant was saved as the SV-40 sample. To remove the cell debris from the collected virus suspension, each suspension was centrifuged at $450\times g$ for 10 min. After removing the debris, the resulting stock viruses were aliquoted and stored at -80 °C until use.

Determination of Viral Infectivity The infectious titer of virus suspension was determined using indicator cells. Poliovirus and porcine parvovirus were introduced into Vero cells and ESK cells, respectively.[13] The cells were seeded in a 96-well microplate (Asahi Technoglass Co., Ltd., Tokyo) at a density of 2×10^5 to 3×10^5 cells per well in culture medium. They were then cultured at 37 °C, for 2 d. Various concentrations of Phx-1 or Phx-2 solution [final concentration: 0 μg/ml (DMSO alone), 0.25, 0.5, 1 and 2 μg/ml] were then added to the cells in each well, and these were subsequently incubated for 1 h. After 1 h, the supernatant was removed from the well by an aspirator. At this time, poliovirus or porcine parvovirus which had been serially diluted with α-MEM to obtain a 50% tissue culture infectious dose ($TCID_{50}$, defined as dilution ratio of the virus to generate 50% disruption of the cells), as performed conventionally,[2] was added to Vero cells or ESK cells, respectively, in each well. Cell cultures were incubated for 1 h at 37 °C. Post infection $TCID_{50}$ cultures were then fed with α-MEM containing various concentrations of Phx-1 or Phx-2 [final concentration: 0 (DMSO alone), 0.25, 0.5, 1 and 2 μg/ml] and were incubated at 37 °C for 2 or 3 d.

After that period, the disruption of Vero cells or ESK cells was examined by the method described by Satoh *et al.*,[14] and the infectivity of poliovirus or porcine parvovirus to these cells was estimated. The estimation of the viruses SV-40, HSV-1, Sindbis virus and VSV was essentially in agreement with the method described by Satoh *et al.*[14]

Effects of Phx-1 and Phx-2 on Cell Viability We examined the effects of Phx-1 and Phx-2 on the viability of Vero cells, ESK cells, and CV-1 cells in the presence of various concentrations of these phenoxazines and without addition of viruses. There was no significant disruption of these cells at various concentrations of Phx-1 and Phx-2 up to 50 μg/ml, indicating that these phenoxazines do not affect the viability of the cells at the concentrations of used to examine the viruses.

RESULTS AND DISCUSSION

We initially studied the effects of Phx-1 and Phx-2 on the proliferation of poliovirus, a non-enveloped and single strand RNA virus, inoculated to Vero cells. Since $TCID_{50}$ is defined as the dilution ratio of the virus to generate 50% disruption of the cells, a lower value of $TCID_{50}$ means that the viral proliferation is being suppressed in the host cells. We found that

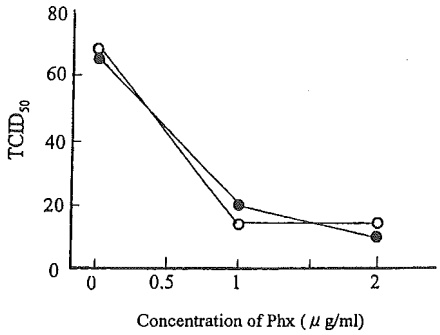

Fig. 2. Antiviral Effects of Phx-1 and Phx-2 on Porcine Parvovirus

The infectious titer of porcine parvovirus suspension was determined using ESK cells, as described in Materials and Methods. Antiviral effects of Phx-1 (●) or Phx-2 (○) were expressed by $TCID_{50}$ (defined as dilution ratio of the virus to generate 50% disruption of the cells) at different concentrations of these phenoxazines (μg/ml of Phx-1 or Phx-2).

$TCID_{50}$ of poliovirus was decreased according to the increase in the concentrations of Phx-1 or Phx-2 (Table 1). Namely, Phx-1 suppressed the proliferation of poliovirus inoculated to Vero cells at all concentrations tested between 0.25 μg/mg and 2 μg/ml, and reached maximal antiviral activity at 1 μg/ml. Phx-2 also inhibited the proliferation of poliovirus inoculated to Vero cells at 2 μg/ml (Table 1). Such inhibition was observed when the cells were treated with Phx-1 or Phx-2 for 1 h and then inoculated with poliovirus. On the contrary, the proliferation of poliovirus was not suppressed by Phx-1 or Phx-2 when Vero cells were inoculated with the virus together with various concentrations of Phx-1 or Phx-2 (data not shown). These results may be explained by the facts that these phenoxazines do not exert virucidal activity against poliovirus directly, but some mechanisms preventing the attachment or the intracellular proliferation of poliovirus in the host cells, are apparently revoked during 1 h incubation of the host cells with Phx-1 or Phx-2. The detailed biochemical changes in the host cells are not yet clear.

Figure 2 shows the inhibitory effects of Phx-1 and Phx-2 against porcine parvovirus, a non-enveloped and single strand DNA virus, as determined by the changes in $TCID_{50}$. These phenoxazines showed antiviral effects on porcine parvovirus at 1 μg/ml and 2 μg/ml. Such inhibition was observed when the cells were treated with Phx-1 or Phx-2 for 1 h and then inoculated with porcine parvovirus. However, Phx-1 or Phx-2 did not exert antiviral effects on porcine parvovirus when ESK cells were inoculated with the virus together with Phx-1 or Phx-2 (data not shown).

We studied the effects of Phx-1 and Phx-2 on various representative viruses such as SV-40 (non-enveloped, double strand DNA), HSV-1 (enveloped, double strand DNA), Sindbis virus (enveloped, single and plus strand RNA), and VSV (enveloped, single strand RNA). Table 2 summarizes the

Table 2. Antiviral Activity of Phx-1 and Phx-2 on Various Species of Viruses

Type of virus	Name of virus	Antiviral activity[a]	
		Phx-1	Phx-2
sDNA, envelope (−)	Porcine parvovirus	+	+
dDNA, envelope (−)	Simian virus 40	−	−
dDNA, envelope (+)	Herpes simplex virus-1	−	−
sRNA, envelope (−) (plus strand)	Poliovirus	+	+
sRNA, envelope (+) (plus strand)	Sindbis virus	−	−
sRNA, envelope (+) (minus strand)	Vesicular stomatitis virus	−	−

a) $TCID_{50}$ was estimated as described in Materials and Methods. Then, the antiviral activity was expressed by + or −, where + shows "effective" at the concentration of Phx-1 or Phx-2 between 0.25 and 20 μg/ml, and − shows "not effective" at these concentrations.

inhibitory effects of Phx-1 and Phx-2 on these viruses, in comparison with poliovirus and porcine parvovirus. Although Phx-1 and Phx-2 showed antiviral activity against poliovirus and porcine parvovirus, these phenoxazines did not inhibit the proliferation of SV-40, HSV-1, Sindbis virus or VSV in the host cells. Therefore, it may be conceivable that non-enveloped and single strand RNA virus (coxackie virus, ECHO virus, hepatitis virus A, encephalomyocarditis virus *etc.*) or non-enveloped and single strand DNA virus (B19 virus, adeno-associated virus 2 *etc.*) may be inhibited by Phx-1 and Phx-2 as well. Increased amounts of interferon is not possible, because the inhibition of proliferation of viruses was restricted only to poliovirus and porcine parvovirus (Table 2). These views should be assessed by further examinations.

Tang *et al.*[15] reported that hypericin, a derivative of emodin exerts antiviral activity against enveloped viruses such as HSV-1, influenza virus A and Mo-Mul V, but not against the non-enveloped viruses poliovirus and adenovirus, at concentrations of 1.56 to 25 μg/ml. On the other hand, our results showed that Phx-1 and Phx-2 exerted antiviral activity only against poliovirus and porcine parvovirus (Table 1, Fig. 2). Concerning the chemical structure of emodin (1,3,8-trihydroxy-6-methylanthraquinone) and Phx-1, emodin is analogous to Phx-1, because emodin and Phx-1 (Fig. 1) are tricyclic chromophores with the methyl group at the same position, however, the former is a semiquinone type producing active oxygens,[16] while the latter is a non-semiquinone type. Such similarity and differences in the chemical structure of these compounds may be reflected to the differences in biological actions between hypericin and Phx-1 or Phx-2.

Acknowledgments The present research was supported by funds from the Ito Foundation and from High-Tech Research Project for Private Universities: matching fund subsidy from the Ministry of Education, Culture, Sports, Science and Technology, Japan (2002—2006).

REFERENCES

1) Schaffer H. J., Beauchamp L., de Miranda P., Elion G. B., Bauer D. J., Collins P., *Nature* (London), **272**, 583—585 (1978).
2) Schmidtke M., Schnittler U., Jahn B., Dahse H., Stelzner A., *J. Virol. Methods*, **95**, 133—143 (2001).
3) Tomoda A., Yamaguchi J., Kojima H., Amemiya H., Yoneyama Y., *FEBS Lett.*, **196**, 44—48 (1986).
4) Tomoda A., Hamashima H., Arisawa M., Kikuchi T., Tezuka Y., Koshimura S., *Biochim. Biophys. Acta*, **1117**, 306—314 (1992).
5) Tomoda A., Arisawa M., Koshimura S., *J. Biochem.* (Tokyo), **110**, 1004—1007 (1991).
6) Mori H., Honda K., Ishida R., Nohira T., Tomoda A., *Anti-Cancer Drugs*, **11**, 653—657 (2000).
7) Koshibu-Koizumi J., Akazawa M., Iwamoto T., Takasaki M., Mizuno F., Kobayashi R., Abe A., Tomoda A., Hamatake M., Ishida R., *J. Cancer Res. Clin. Oncol.* **128**, 363—368 (2002).
8) Akazawa M., Koshibu-Koizumi J., Iwamoto T., Takasaki M., Nakamura M., Tomoda A., *Tohoku J. Exp. Med.*, **196**, 185—192 (2002).
9) Gao S., Takano T., Sada K., He J., Noda C., Hori-Tamura N., Tomoda A., Yamamura H., *Br. J. Pharmacol.*, **137**, 749—755 (2002).
10) Enoki E., Sada K., Qu X., Kyo S., Shahjahan Miah S. M., Hatani T., Tomoda A., Yamamura H., *J. Pharm. Sci.*, **94**, 329—333 (2004).
11) Iwata A., Yamaguchi A., Sato K., Izumi R., Tomoda A., *Tohoku J. Exp. Med.*, **200**, 161—165 (2003).
12) Kawamura H., Fujita T., Imada T., *Nippon Juigaku Zasshi*, **50**, 803—808 (1988).
13) Johnson K. L., Sarnow S. P., *J. Virol.*, **65**, 4341—4349 (1991).
14) Satoh K., Iwata A., Murata M., Hikata M., Hayakawa T., Yamaguchi T., *J. Virol. Methods*, **114**, 111—119 (2003).
15) Tang J., Colacino J. M., Larsen S. H., Spitzer W., *Antiviral Res.*, **13**, 313—326 (1990).
16) Huang H. C., Chu S. H., Chao P. D. L., *Eur. J. Pharmacol.*, **198**, 211—213 (1991).

Available online at www.sciencedirect.com
SCIENCE DIRECT®
Biologicals 32 (2004) 139–146
BIOLOGICALS
www.elsevier.com/locate/biologicals

An improved method for detection of replication-competent retrovirus in retrovirus vector products

Eriko Uchida[a,*], Koei Sato[b], Akiko Iwata[b], Akiko Ishii-Watabe[a], Hiroyuki Mizuguchi[a], Mikio Hikata[c], Mitsuhiro Murata[c], Teruhide Yamaguchi[a], Takao Hayakawa[a]

[a]*National Institute of Health Sciences, 1-18-1 Kamiyoga, Setagaya-ku, Tokyo 158-8501, Japan*
[b]*Institute of Saitama Red Cross Center, 398-1 O-aza-narashinden, Kumagaya, Saitama 368-0806, Japan*
[c]*JSR Corporation, Tsukuba Research Laboratories, Miyukigaoka 25, Tsukuba, Ibaraki 305-0841, Japan*

Received 20 February 2004; accepted 19 August 2004

Abstract

Contamination by replication-competent retrovirus (RCR) is one of the most important safety issues of retrovirus vector products for gene therapy clinical research. To improve the sensitivity of RCR detection and to shorten the assay period, we have developed a novel RCR detection method (infectivity RT-PCR method) based on real-time quantitative reverse transcription-polymerase chain reaction (RT-PCR) in combination with virus infection and a novel virus concentration method using polyethyleneimine (PEI)-conjugated magnetic beads. In this method, permissive cells were infected with RCR samples, and amplified RCR in the culture supernatants was adsorbed by PEI-beads. Then RCR RNA extracted from PEI-beads was quantified by real-time RT-PCR. We demonstrated that 1 infectious unit (iu) of RCR spiked in 10^6 cfu/ml of vector products could be detected within 3 days, and the sensitivity for viral detection was increased 3- to 10-fold compared with the direct S + L− assay. By this method, the presence of retroviral vector interfered with RCR detection only slightly. In conclusion, infectivity RT-PCR conducted in conjunction with virus concentration using PEI-beads can detect RCR more sensitively and rapidly than the conventional infectivity assay.

1. Introduction

Retrovirus vectors are widely used in human gene therapy to treat genetic diseases, cancer, and other conditions. The retroviral vector products currently used in gene therapy clinical researches are replication-defective retroviruses, and the primary safety concern associated with the use of retroviral vector products is contamination by replication-competent retrovirus (RCR). RCR is the major risk factor for insertional mutagenesis, and exposure to retrovirus vector contaminated with a high titer of RCR has been shown to lead to lymphoma in rhesus monkeys [1].

The most likely source of RCR is the vector-packaging sequence. Since RCR can arise by homologous recombination during the production of retroviral vector supernatants, sensitive assays for the screening of RCR in vector products are required. The U.S. Food and Drug Administration (FDA) has developed guidelines for testing of RCR in clinical grade vectors and transduced cells, as well as for monitoring patients

Abbreviations: RCR, replication-competent retrovirus; RT-PCR, reverse transcription-polymerase chain reaction; PEI, polyethyleneimine; iu, infectious units; cfu, colony forming units; MLV, murine leukemia virus; AMLV, amphotropic MLV.

* Corresponding author. Tel./fax: +81 3 3700 9217.
E-mail address: uchida@nihs.go.jp (E. Uchida).

1045-1056/04/$30.00
doi:10.1016/j.biologicals.2004.08.002

treated with gene therapy protocols [2]. The FDA guidelines recommend that retrovirus vector products be tested for the presence of RCR by inoculation and passage of the test sample with a permissive cell line for a minimum of 5 passages in order to amplify any potential RCR present, followed by subsequent testing with an appropriate indicator cell assay. The PG-4 S + L− focus-forming assay and the marker rescue assays have been routinely used for the detection of RCR [3–7]. However, these conventional cell-based assays are known to have several disadvantages: the assays take a long time (weeks), visual evaluation of the results requires skill and is labor intensive, and the limited dynamic range requires many dilutions. Therefore, there is need for a more sensitive and rapid quantitative detection method for RCR.

Polymerase chain reaction (PCR) is a highly sensitive method for the detection of viral genomes [8]. It has been reported that PCR assays were capable of detecting one or more copies of RCR provirus in 500,000 cells [9]. PCR-based assay for RCR is used for biosafety monitoring of transduced cells with retroviral vectors [10] and of patients receiving retroviral gene therapy [9,11].

Moreover, the recently developed fluorescence-based real-time quantitative reverse transcription-PCR (RT-PCR) assay allows precise quantification of RNA genomes. Since quantitative RT-PCR can be performed in a short time with a wide dynamic range and high throughput, it is expected to be particularly suitable for quantifying RCR in viral stocks with high sensitivity. However, the PCR-based assay detects not only infectious virus genomes. In previous studies, PCR-based assays detected viral DNA fragments derived from packaging cell lines contaminated into retrovirus vector supernatants and caused false-positive findings [12,13]. Therefore, when quantitative RT-PCR is used for RCR detection, some process is required to distinguish infectious RCR RNA and viral DNA fragments prior to the quantitative RT-PCR assay. Infection of RCR into a permissive cell line is suitable for this purpose, because infectious RCR selectively replicates in cells without replication of viral DNA fragments and retrovirus vectors.

In addition, if RCR could be concentrated when preparing the sample for quantitative RT-PCR, it is expected that the sensitivity of RCR genome detection could be improved. In a previous study, our group demonstrated that polyethyleneimine (PEI)-conjugated magnetic beads efficiently adsorbed many types of viruses, with the exception of some non-enveloped viruses, and this novel virus concentration method using PEI-beads enhanced the sensitivity of virus detection by both PCR and RT-PCR [14].

In the present study, we have established a novel RCR detection method based on infectivity RT-PCR. Infectivity RT-PCR is a hybrid method that attempts to combine the best features of infectivity assays and quantitative RT-PCR. Samples are allowed to amplify in cell culture, as in conventional assays. Replication-competent retrovirus is quantified by real-time quantitative RT-PCR rather than by counting focuses. In addition, we applied a novel virus concentration method using PEI-beads to concentrate RCR in culture supernatants before quantitative RT-PCR. We demonstrated that this novel method could detect RCR more sensitively and rapidly than the conventional culture assays.

2. Materials and methods

2.1. Virus and cells

Hybrid Moloney/amphotropic *Murine leukemia virus* (MLV) obtained from ATCC (Manassas, VA; VR-1450; virus titer: $6.9 \pm 2.0 \times 10^7$ infectious unit (iu)/ml) was used as the RCR Reference Material. This hybrid virus, which was established by both the FDA and ATCC as an MLV RCR Reference Material, consists of Moloney MLV with a substitution of the *env* coding region from the 4070A strain of amphotropic MLV (AMLV), and represents a typical recombinant virus that could be generated in a retroviral packaging cell line containing coding sequences for an AMLV *env* [2].

Mus dunni cells (CRL-2017) and cat fibroblast PG-4 (S + L−) cells (CRL-2032) were obtained from ATCC. NIH/3T3 cells (JCRB0615) were obtained from the Japanese Cancer Research Resource Bank (Tokyo, Japan). ΨCRIP-P131 cells (RCB1088) were obtained from the RIKEN Cell Bank (Tsukuba, Japan). *M. dunni* cells and PG-4 (S + L−) cells were maintained in McCoy's 5A medium with 10% fetal calf serum (FCS). NIH/3T3 cells and ΨCRIP-P131 cells were maintained in Dulbecco's modified Eagle's medium (DMEM) supplemented with 10% calf serum.

2.2. Preparation of recombinant retrovirus vector

The retrovirus vector plasmid pLEGFP-N1 (Clontech, Palo Alto, CA) contains the enhanced green fluorescent protein (EGFP) and neomycin resistance gene. ΨCRIP-P131 cells which contain the *gag/pol* gene of Moloney MLV and *env* gene of 4070A in different expression vectors were used as a high titer retrovirus vector-packaging cell line. ΨCRIP-P131 cells (1×10^6 cells) were transfected with pLEGFP-N1 (2 μg) by Effectene Transfection Reagent (Qiagen, Hilden, Germany). Two days after transfection, cells were trypsinized and replated. The next day, Geneticin (GIBCO-BRL, Grand Island, NY; final concentration 1 mg/ml) were added to each dish and cultured for an additional 2 weeks. Eighteen clones of neomycin-resistant cells were picked up, and a clone (ΨCRIP-LEGFP1) which showed the

highest EGFP expression when the NIH/3T3 cells were infected with the culture supernatants of cloned cells was used as a line of retrovirus vector-producing cells. For the preparation of retrovirus vector sample, ΨCRIP-LEGFP1 cells were cultured to subconfluence, the medium was replaced with fresh medium, and after 24 h of culture, the culture supernatants were collected as retrovirus vector samples (vector titer: 1×10^6 cfu/ml). Vector supernatants were stored at −80 °C until use.

2.3. RCR concentration by PEI-beads

PEI-beads were made by coupling of PEI (MW 70,000; Wako Pure Chemical Inc., Tokyo, Japan) with magnetic beads (IMMUTEX-MAG™; mean diameter: 0.8 μm; JSR Inc., Tokyo, Japan) by the 1-ethylene-3-(3-dimethylaminopropyl)carbodiimide coupling method as described previously [14]. RCR concentration using PEI-beads was done as follows: various dilutions of RCR solution were prepared from RCR Reference Material diluted with DMEM. Then 1 or 10 ml of each RCR dilution was incubated with 100 μl of PEI-beads for 10 min at room temperature. Then the complexes of virus and PEI-beads were trapped by a magnetic field (for 1 ml: Magnetic Trapper™, Toyobo Co., Tokyo, Japan; for 10 ml: Dynal MOC-1™, Dynal AS, Oslo, Norway). The virus genome was extracted from the PEI-beads adsorbed fraction (the whole volume) or unadsorbed supernatant (100 μl) with an SMI-TEST EX R&D Kit (Genome Science Laboratories, Fukushima, Japan). Extracted nucleic acids were dissolved in 50 μl of DNase/RNase-free distilled water, and 10 μl of this solution was used for the quantitative RT-PCR reaction.

2.4. Real-time quantitative RT-PCR

The real-time quantitative RT-PCR for RCR was monitored on an ABI PRISM 7000 Sequence Detection System (Applied Biosystems, Foster City, CA). The reaction was carried out in a 50 μl reaction mixture containing 10 μl of extracted sample, 1 μM each of the forward and reverse primer, 0.2 μM of TaqMan probe, and 25 μl of TaqMan One-Step RT-PCR Master Mix Reagents with 1.25 μl of 40× MultiScribe and RNase Inhibitor (Applied Biosystems). The reaction conditions were as follows: the viral RNA was reverse-transcribed into cDNA for 30 min at 48 °C, then heat-inactivated for 10 min at 95 °C; PCR was then performed for 50 cycles of 15 s at 95 °C and 1 min at 60 °C. Standard curves were generated from RCR RNA extracted from RCR Reference Material in each RT-PCR assay and validated using linear regression analysis. The RCR genomes were quantified in infectious units (iu). One infectious unit of RCR measured by quantitative RT-PCR means that the sample contains virus genome RNA equivalent to 1 iu of RCR Reference Material. The sequences of the primer pair and the probe used were as follows: forward primer (AMLVenv-1018F): 5′-GCG GTC GTG GGC ACT TAT A-3′; reverse primer (AMLVenv-1082R): 5′-TGT TGG GAA GTG GCC GTA C-3′; TaqMan probe (AMLVenv-1040TM): 5′-(FAM)-ATC ATT CCA CCG CTC CGG CCA-(TAMRA)-3′. These sequences were designed to detect the *env* gene of 4070A AMLV using Primer Express Ver 1.0 Software (Applied Biosystems). The amplified product is predicted to be 64 base pairs (bp) in length.

2.5. Amplification of RCR by culture cells

M. dunni cells were plated in 60-mm dishes at 2×10^5 cells/dish and cultured overnight. Culture medium was replaced with 1 ml of polybrene solution (16 μg/ml) as well as 1 ml of virus solution and incubated for 4 h at 37 °C. Cells were washed with 1 ml of medium 3 times and incubated with 5 ml of fresh culture medium. Culture supernatants were collected at the indicated days for RCR concentration using PEI-beads and detected by quantitative RT-PCR.

2.6. S + L− focus-forming assay

The PG-4 cells were plated in 6-well plates at a concentration of 2×10^5 cells/well and incubated at 37 °C in 5% CO_2 overnight. On the day of infection, the medium was discarded, 1 ml of DEAE-Dextran (20 μg/ml in medium) was added to each well, and the cells were incubated for 30 min at 37 °C. Then 1 ml of test sample was added to each well and the cells were incubated for 2 h at 37 °C. Finally, the samples were replaced with 2 ml of fresh culture medium and cultured at 37 °C in 5% CO_2. Foci of transformed cells were examined microscopically on day 3 and day 7.

3. Results

3.1. Detection of RCR RNA by real-time quantitative RT-PCR

We first established the detection method of RCR RNA by real-time quantitative RT-PCR. Serial log dilutions of RCR solution were prepared, and viral genome RNA extracted from 100 μl of each RCR solution was analyzed by TaqMan quantitative RT-PCR. Forward and reverse primers as well as the TaqMan probe used for the detection of RCR were designed to detect the AMLV *env* sequence that exists in the RCR genome but not in the retroviral vector sequence (Fig. 1). Fig. 2 shows the standard curve generated from an amplification plot of the quantitative RT-PCR assay for RCR. A linear relationship was observed between the threshold cycle (C_T, the PCR cycle at which the

fluorescence of amplification first exceeds baseline) and the log-transformed input retroviral RNA genomes. The linearity of the standard curve was obtained at a range of 10^{-1}–10^{6} iu of RCR in 100 μl of the sample with a correlation coefficient of 0.998. The standard curve was reproducible for repeated assay (data not shown). Since C_T could not be calculated from virus solutions having concentrations below 0.1 iu, the detection limit of the quantitative RT-PCR for RCR was 0.1 iu.

3.2. Concentration of RCR by PEI-beads

In order to detect very low titers of RCR in the culture supernatants of infected cells, we tried to concentrate retrovirus particles using PEI-beads. One and 10 ml of RCR solution (10^{-5} dilution of RCR in DMEM) were incubated with 100 μl of PEI-beads, and fractionated into the PEI-beads adsorbed fraction and the unadsorbed supernatant fraction. Viral genome RNA extracted from each fraction was applied to RT-PCR and analyzed by agarose gel electrophoresis. As shown in Fig. 3A, RCR *env* RNA was detected by RT-PCR from the PEI-beads adsorbed fraction but not from the unadsorbed supernatant, indicating that RCR was efficiently adsorbed in the PEI-beads. When the starting volume of virus solution used for concentration was increased from 1 to 10 ml, the amounts of RCR RNA obtained in the PEI-beads adsorbed fraction were increased without any change in the unadsorbed fraction. To analyze the concentration of virus with PEI-beads quantitatively, serial log dilutions of RCR solution were fractionated with PEI-beads, and the amounts of RCR RNA in the adsorbed fraction and the unadsorbed fraction were quantified by real-time RT-PCR (Table 1, Fig. 3B). When solutions containing low concentrations of RCR were applied to PEI-beads, all of the retrovirus particles in the viral solutions were efficiently collected in the PEI-beads fraction. On the other hand, when a solution containing high concentration of RCR was applied to the PEI-beads, unadsorbed

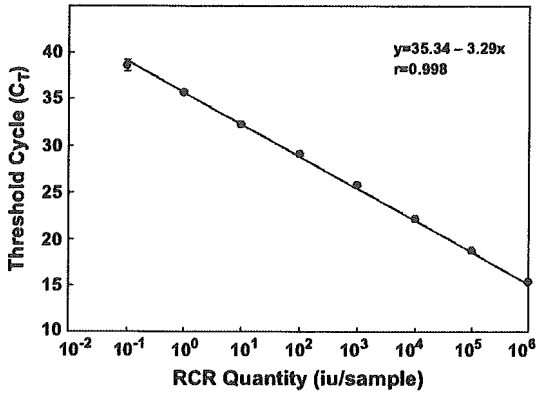

Fig. 2. Standard curve for the determination of RCR quantity generated from an amplification plot of real-time quantitative RT-PCR. Serial dilutions of RCR solution were analyzed by quantitative RT-PCR. A standard curve was generated from the amplification plot of RCR using real-time quantitative RT-PCR. The correlation coefficient is 0.998. Data are the mean ± S.D. (n = 3).

viruses were detected in the supernatant (Table 1). As a result, RCR treated with PEI-beads were maximally concentrated about 10-fold from 1 ml of virus solution and 100-fold from 10 ml of virus solution compared to direct extraction from 100 μl of original virus solutions, and at the same time, the assay sensitivity was increased about 10- and 100-fold, respectively (Table 1, Fig. 3B). These results clearly demonstrated that PEI-beads efficiently adsorbed RCR, and that this novel virus concentration method is useful for improving the sensitivity and lowering the limits of RCR detection.

3.3. Amplification of RCR in cell culture for infectivity RT-PCR

For the screening of RCR in retrovirus vector products, it is necessary to detect very less amounts of RCR among large amounts of retrovirus vectors. In our preliminary study, however, viral *env* DNA sequences derived from a packaging cell line were used to

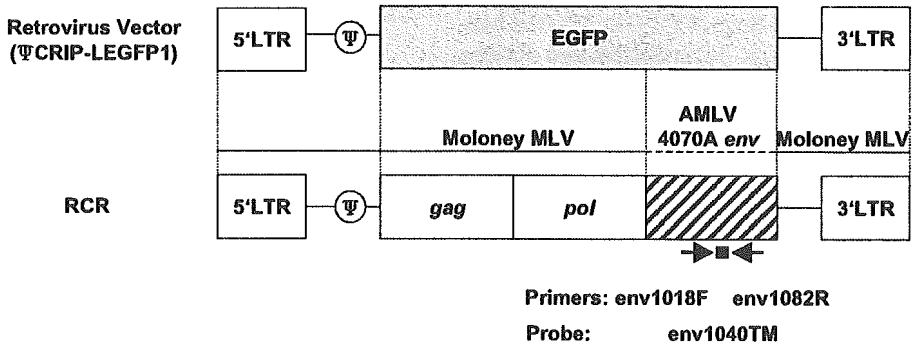

Fig. 1. Structure of RCR and retrovirus vector used in this study. The open bars represent Moloney MLV genome, the gray bar represents the expression cassette for the EGFP gene, and the striped bar represents the AMLV 4070A *env* gene. Black arrows and a small black square underneath the RCR genome indicate the location of the primers and a probe for RCR detection, respectively.